

Integral cross sections for electron scattering by ground state Ba atoms

D. V. Fursa^{†*}, S. Trajmar[‡], I. Bray[†], I. Kanik[‡],

G. Csanak[§], R.E.H. Clark[§], and J. Abdallah Jr.[§]

[†] *The Flinders University of South Australia, G.P.O. Box 2100, Adelaide 5001, Australia*

[‡] *Jet Propulsion Laboratory, California Institute of Technology, Pasadena, CA, USA*

[§] *Los Alamos National Laboratory, University of California, Los Alamos, NM 887545, USA*

(June 22, 2021)

Abstract

We have used the convergent close-coupling method and a unitarized first-order many-body theory to calculate integral cross sections for elastic scattering and momentum transfer, for excitation of the $5d^2\ ^1S$, $6s6p\ ^1P_1$, $6s7p\ ^1P_1$, $6s8p\ ^1P_1$, $6s5d\ ^1D_2$, $5d^2\ ^1D_2$, $6s6d\ ^1D_2$, $6p5d\ ^1F_3$, $6s4f\ ^1F_3$, $6p5d\ ^1D_2$, $6s6p\ ^3P_{0,1,2}$, $6s5d\ ^3D_{1,2,3}$, and $6p5d\ ^3D_2$ states, for ionization and for total scattering by electron impact on the ground state of barium at incident electron energies from 1 to 1000 eV. These results and all available experimental data have been combined to produce a recommended set of integral cross sections.

34.80.Bm, 34.80.Dp

Typeset using REVTeX

*electronic address: dmitry.fursa@flinders.edu.au

I. INTRODUCTION

A great deal of interest and need has developed in recent years for electron collision cross sections involving Ba atoms. In the applications area, these cross sections are needed for modelling the behavior of Ba vapor lasers [1–4], discharge lamps [5], plasma switches [6], and various planetary ionospheres [7–12], where Ba has often been used as a trace element for diagnostic purposes. On the academic side, benchmark laboratory cross sections are needed for testing various theoretical approximations and calculational methods hoping to predict these cross sections.

The experimental data base, available at the present time, is rather limited both in the electron impact energy range and the scattering channels. Line emission cross sections for the $(6s6p\ ^1P_1 \rightarrow 6s^2\ ^1S_0)$ at 5535 Å [$Q_{emiss}(6s6p\ ^1P_1)$] were determined by Chen and Gallagher [13] in the 2.3 to 1497.0 eV impact energy range. They claimed an uncertainty of $\pm 5\%$. Since the $6s6p\ ^1P_1$ level decays predominantly (99.7%) to the ground state, the measured line emission cross sections are equivalent (within the experimental error limits) to the apparent $6s6p\ ^1P_1$ level excitation cross sections [$Q_{App}(6s6p\ ^1P_1)$] and they differ from the electron impact excitation cross sections [$Q(6s6p\ ^1P_1)$] by the cascade contributions. (See e.g. Trajmar and Nickel [14] for the definitions of these cross sections.) Cascade corrections, only available from theory, can be applied to the data of Chen and Gallagher and the resulting $Q(6s6p\ ^1P_1)$ values represent the most reliable electron scattering cross sections available for Ba at the present time. Jensen *et al.* [15] and Wang *et al.* [16] determined relative cross sections for elastic scattering (Q_{elas}) and momentum transfer (Q_M) at a few impact energies. Jensen *et al.* [15] also obtained some cross section results for excitation of the $6s5d\ ^1D_2$ level [$Q(6s5d\ ^1D_2)$]. In these cases, the relative cross sections were normalized by an estimated cascade correction applied to the Chen and Gallagher $Q_{App}(6s6p\ ^1P_1)$ values to obtain $Q(6s6p\ ^1P_1)$ values which in turn were used to normalize Q_{elas} , Q_M , and $Q(6s5d\ ^1D_2)$. Total ionization cross section (Q_i) in the threshold to 600 eV range have been reported by Dettmann and Karstensen [17] and by Vainshtein *et al.* [18] from the threshold to 200 eV.

Total electron scattering cross sections (Q_{Tot}) were measured by Romanyuk *et al.* [19] in the 0.1 to 10 eV range.

There is a larger data base available from calculations. Elastic scattering cross sections were calculated by Gregory and Fink [20] in the 100 to 1500 eV range. (numerical solutions of the Dirac equation), by Fabrikant [21] at impact energies ranging from 6 eV to 35 eV (non-relativistic close-coupling approximation), by Yuan and Zhang from 0.01 eV to 5.0 eV (quasirelativistic static-exchange formalism) [22] and from 0.04 eV to 150 eV (Hartree-Fock method with relativistic corrections) [23], by Szmytkowski and Sienkiewicz [24] in the 0.2 eV to 100 eV region (relativistic polarized-orbital approximation) and by Kelemen *et al.* [25] from 0.1 to 200 eV (using phenomenological complex optical potential). Szmytkowski and Sienkiewicz [24] and Kelemen *et al.* [25] as well as Gribakin *et al.* [26] (Hartree-Fock approximation with correlation corrections, from zero to 2.5 eV) have reported momentum transfer cross sections. As far as inelastic scattering is concerned, $Q(6s6p\ ^1P_1)$ results were obtained by Fabrikant [21] from threshold to 35 eV (non-relativistic two-state close-coupling approximation), by Clark *et al.* [27] from 5 eV to 100 eV (unitarized distorted-wave approximation, UDWA and first order many-body theory, FOMBT), and Srivastava *et al.* [28,29] from 20 to 100 eV (relativistic distorted-wave approximation, RDWA). Srivastava *et al.* also reported $Q(6s6p\ ^3P_1)$ and $Q(6s5d\ ^1D_2)$ and $Q(6s5d\ ^3D_{1,2,3})$ values. Q_{Tot} results in the 10 to 200 eV range were given by Kelemen *et al.* [25]. Very recently the non-relativistic convergent close-coupling (CCC) method was applied by Fursa and Bray [30,31] to obtain Q_{elas} , Q_M , $Q(6s6p\ ^3P_1)$, $Q(6s5d\ ^1D_2)$ and $Q_{\text{App}}(6s6p\ ^1P_1)$ results in the 1 to 897 eV range.

The present work represents a substantial extension of CCC and UFOMBT calculations to cover all scattering channels which we consider important for practical applications over a wide range of impact energies. Comparison of these theoretical results with fragmentary experimental data allows us to recommend a reliable and consistent cross section data set which should be satisfactory for most modelling calculations. We found very good agreement between the CCC results and experiment and therefore in our recommendations relied heavily on the CCC data.

II. CALCULATIONAL METHODS

A. CCC method

The application of the CCC method to calculation of electron scattering from barium has been discussed elsewhere, see Refs. [31] and [32] for details. Briefly, barium target states are described by a model of two valence electrons above an inert Hartree-Fock core. We have used configuration interaction (CI) expansion technique to obtain barium wave functions. One-electron orbitals used in CI expansion have been obtained by diagonalizing Ba^+ Hamiltonian in a Sturmian (Laguerre) basis. In Table I we compare energies for the states relevant to the present study with experimental data and give a set of the dominant configurations for each state. We find a very good agreement between our results and experiment and other accurate calculations for energy levels and oscillator strengths [31]. The barium target states obtained this way provide not only an accurate representation of the barium discrete spectrum but allow also for square-integrable representation of the target continuum. This allows for coupling to the ionization channels in the scattering calculations. These calculations use barium target states in order to perform expansion of the total wave function and formulate a set of close-coupling equations. These equations (for the T matrix) are formulated and solved in momentum space.

The CCC method is formulated as a purely non-relativistic theory in both target structure and electron scattering calculations. In order to compare results from the non-relativistic CCC calculations with experiment, we have used a technique essentially identical with the transformation scheme described by Saraph [33]. Namely, we first transform the non-relativistic CCC scattering amplitudes $f_{\pi_f s_f l_f m_f, \pi_i s_i l_i m_i}^S$ to the amplitudes describing transitions between fine-structure levels J_f and J_i ,

$$f_{\pi_f J_f M_f, \pi_i J_i M_i}^{\sigma_f, \sigma_i}(s_f l_f \gamma_f, s_i l_i \gamma_i) = \sum_{m_f, q_f, m_f, q_f, S} C_{l_f m_f, s_f q_f}^{J_f M_f} C_{\frac{1}{2} \sigma_f, s_f q_f}^{SM_S} C_{l_i m_i, s_i q_i}^{J_i M_i} C_{\frac{1}{2} \sigma_i, s_i q_i}^{SM_S} f_{\pi_f s_f l_f m_f, \pi_i s_i l_i m_i}^S(\gamma_f, \gamma_i). \quad (1)$$

Here S is total spin, and π_f (π_i), s_f (s_i), l_f (l_i) and m_f (m_i) are the final (initial) target state

parity, spin, orbital angular momentum is and its projection on the Z-axis of the collision frame, respectively. The final (initial) projectile spin projection on the Z-axis of the collision frame is indicated as σ_f (σ_i), and the index γ distinguishes states with the same orbital angular momentum, spin and parity. The above amplitudes are used to form amplitudes in the intermediate coupling scheme

$$F_{\pi_f J_f M_f, \pi_i J_i M_i}^{\sigma_f, \sigma_i}(\beta_f, \beta_i) = \sum_{s_f, l_f, s_i, l_i} \sum_{\gamma_f, \gamma_i} C_{\gamma_f}^{\beta_f} C_{\gamma_i}^{\beta_i} f_{\pi_f J_f M_f, \pi_i J_i M_i}^{\sigma_f, \sigma_i}(s_f l_f \gamma_f, s_i l_i \gamma_i), \quad (2)$$

where the index β distinguishes target states with the same total angular momentum J and parity π . We obtain mixing coefficients C_{γ}^{β} by diagonalizing the Breit-Pauli Hamiltonian (only one-body spin-orbit term is used) in the basis of the barium target states obtained from the non-relativistic barium structure calculation. Note that the dependence of the scattering amplitudes in (1) and (2) on the electron spherical angles θ and φ is implicit.

Amplitudes (2) are used to calculate the semi-relativistic integrated cross sections:

$$Q_{\text{fs}} = \frac{k_f}{2(2J_i + 1)k_i} \sum_{M_f, M_i, m_f, m_i} \int d\Omega |F_{\pi_f J_f M_f, \pi_i J_i M_i}^{\sigma_f, \sigma_i}(\beta_f, \beta_i)|^2. \quad (3)$$

The subscript ‘‘fs’’ (fine-structure) indicates that the cross section is calculated with an (approximate) account of relativistic corrections.

Scattering on a singlet initial state allows for significant simplification in Eq. (3). Symmetry relations of the scattering amplitudes (1)

$$f_{\pi_f J_f M_f, \pi_i J_i M_i}^{\sigma_f, \sigma_i}(s_f l_f \gamma_f, s_i l_i \gamma_i) = -(-1)^{s_f} f_{\pi_f J_f M_f, \pi_i J_i M_i}^{-\sigma_f, -\sigma_i}(s_f l_f \gamma_f, s_i l_i \gamma_i), \quad s_i = 0, \quad (4)$$

ensure that the singlet-triplet terms in Eq. (3) are zero after summation over projectile spin magnetic sublevels m_f and m_i . We have also found that for the target states involved in the present study only one or two terms in Eq. (2) have large mixing coefficients. Together, these allow us to express the cross section defined by (3) in terms of the non-relativistic cross sections Q which are obtained from the non-relativistic amplitudes (1) using Eq. (3). We give below decomposition of the semi-relativistic ICS (3) via non-relativistic cross sections,

$$Q_{\text{fs}}(5d^2 \ ^1S_0) = 0.9635 Q(5d^2 \ ^1S_0) + 0.0339 Q(5d^2 \ ^3P_0) \quad (5a)$$

$$Q_{\text{fs}}(6s6p \ ^3P_1) = 0.9934 Q(6s6p \ ^3P_1) + 0.0058 Q(6s6p \ ^1P) \quad (5b)$$

$$Q_{\text{fs}}(6s5d \ ^1D_2) = 0.9779 Q(6s5d \ ^1D_2) + 0.0220 Q(6s5d \ ^3D_2) \quad (5c)$$

$$Q_{\text{fs}}(6s5d \ ^3D_2) = 0.9779 Q(6s5d \ ^3D_2) + 0.0220 Q(6s5d \ ^1D_2) \quad (5d)$$

$$Q_{\text{fs}}(6s6d \ ^1D_2) = 0.9845 Q(6s6d \ ^1D_2) + 0.0136 Q(6s6d \ ^3D_2) \quad (5e)$$

$$Q_{\text{fs}}(5d^2 \ ^1D_2) = 0.8591 Q(5d^2 \ ^1D_2) + 0.1292 Q(5d^2 \ ^3P_2) \quad (5f)$$

$$Q_{\text{fs}}(6p5d \ ^1D_2) = 0.7774 Q(6p5d \ ^1D_2) + 0.2091 Q(6p5d \ ^3F_2) \quad (5g)$$

$$Q_{\text{fs}}(6p5d \ ^3D_2) = 0.9878 Q(6p5d \ ^3D_2) + 0.0075 Q(6p5d \ ^1D_2) \quad (5h)$$

$$Q_{\text{fs}}(6p5d \ ^1F_3) = 0.9698 Q(6p5d \ ^1F_3) + 0.0291 Q(6p5d \ ^3D_3). \quad (5i)$$

These cross sections typically differ by less than 3% from the corresponding cross sections obtained from Eq. (3). All other target states are well described in the non-relativistic approximation.

B. UFOMBT method

The UFOMBT method used here has been discussed in general and in particular its implementation for Ba by Clark *et al.* [27] and Zetner *et al.* [34].

III. RESULTS AND DISCUSSION

A. Line emission, apparent level excitation and electron impact excitation cross section for the $6s6p \ ^1P_1$ level

At the present time, the most reliable electron collision cross sections for Ba are the 5535 Å line emission cross sections [$Q_{\text{emiss}}(6s6p \ ^1P_1)$] associated with the radiative decay of the electron impact and cascade populated $6s6p \ ^1P_1$ level to the ground $6s^2 \ ^1S_0$ state as measured by Chen and Galagher [13]. The uncertainty claimed for these cross sections is about $\pm 5\%$ over the 2.3 to 1497 eV impact energy range. As mentioned in the Introduction,

for all practical purposes these emission cross sections are equivalent to the apparent level excitation cross sections $[Q_{\text{App}}(6s6p\ ^1P_1)]$ from which the electron impact excitation cross sections $[Q(6s6p\ ^1P_1)]$ can be derived if proper account for the cascade contributions can be made. These cross sections can be used as standards to normalize other electron collision cross sections obtained from relative measurements. Indeed, this procedure was followed by Jensen *et al.* [15] and Wang *et al.* [16] who assumed very approximate cascade contributions. A better estimate of these cascade contributions can be made based on the CCC calculations. We will follow here this latter procedure. In Fig. 1 $Q_{\text{App}}(6s6p\ ^1P_1)$ values measured by Chen and Gallagher and those obtained from the CCC and CC(55) calculations (by adding the direct and cascade contributions) are shown. Fig. 2 shows the calculated cascade contribution. Chen and Gallagher have used the Bethe-Born theory to normalize their relative measurements at high energy. They used the value of the optical oscillator strength $f = 1.59$ a.u. for the $6s^2\ ^1S_0 - 6s6p\ ^1P_1$ transition. This value is now known more accurately, $f = 1.64$ a.u. [35]. We, therefore, have multiplied the cross section values given by Chen and Gallagher by the ratio of the latter and former optical oscillator strengths. The excellent agreement between experiment and the CCC results gives credence to the CCC method and some assurance that the $Q(6s6p\ ^1P_1)$ cross sections from these calculations are reliable. In Fig. 3, we compare these cross sections with those obtained from the Chen and Gallagher $Q_{\text{App}}(6s6p\ ^1P_1)$ and the results obtained from other calculational methods. As can be seen from Fig. 3, the calculational methods converge at higher impact energies (above few hundreds eV) but only the CCC results can be considered reliable at intermediate and low impact energies. The set of recommended cross sections are given in Table II. The apparent cross sections are those of Chen and Gallagher, marginally renormalized by multiplication by 1.03 as discussed above. The ratio of $Q_{\text{cascade}}/Q_{\text{App}}$ has been evaluated using the CCC and CC(55) results. Both recommended cascade Q_{cascade} and direct $Q(6s6p\ ^1P_1)$ cross sections have been obtained from the apparent cross sections with the utilization of the CCC $Q_{\text{cascade}}/Q_{\text{App}}$ ratio.

B. Other inelastic scattering channels

In all UFOMBT calculations except for the excitation of the $6s4f\ ^1F_3$ and the $6p5d\ ^1D_2$ levels the 22 configurational basis set described in Zetner *et al.* [34] was used.

Apparent level excitation and electron impact excitation cross sections for the $6s7p\ ^1P_1$ and $6s8p\ ^1P_1$ levels, obtained from CCC, CC(55) and UFOMBT calculations, are shown in Figs. 4, 5 and 6, 7, respectively. No experimental data or other theoretical results are available for these excitation processes. The recommended cross sections are listed in Table III. These values correspond to the CCC results. No recommended cross sections are given below 5.0 eV since the present implementation of the CCC method is too computationally expensive to study resonance regions.

Electron impact excitation cross sections for the $5d^2\ ^1S_0$ level and 1D_2 levels associated with the $6s5d$, $5d^2$, and $6s6d$ major configurations are given in Figs. 8, 9, 10, and 11, respectively. We did not include the very approximate $Q(6s5d\ ^1D_2)$ values of Jensen *et al.* [15] in Fig. 9. No other results are available and again, we give our recommended cross sections based on the CCC calculations in Table IV.

Other important excitation channels are associated with the $6p5d\ ^1D_2$, $6p5d\ ^1F_3$, $6s4f\ ^1F_3$ and $6p5d\ ^3D_2$ levels. The theoretical results for these cross sections are shown in Figs. 12, 13, 14, and 15, respectively and the recommended values are listed in Table V.

Excitation of triplet levels are given for the $6s6p\ ^3P_J$ ($J = 0, 1$ and 2), $6s5d\ ^3D_J$ ($J = 1, 2$ and 3). Only theoretical cross sections are available and they are shown in Figs. 16-18 and 19-21, respectively. The recommended values are summarized in Table VI.

Comparing CCC and UFOMBT results we generally find good agreement at high incident electron energies. However for a few transitions we observe substantial discrepancies even at high impact energies. For the $6p5d\ ^1F_3$ state this discrepancy is the result of the small, but important difference in the CI mixing coefficients for the $nf6s\ ^1F_3$ configuration. We find that the $nf6s\ ^1F_3$ configuration contributes most to the ICS, specially at high energies. We gave preference to the CCC results in this case, because it is likely that the structure

calculations performed in the UFOBT method has not converged for this state. Similarly, for the $6s5d\ ^3D_2$ level a small difference in the singlet-triplet mixing coefficient between $6s5d\ ^3D_2$ and $6s5d\ ^1D_2$ configurations leads to some differences between CCC and UFOMBT calculations at high energies.

The enormous difference between CCC and UFOMBT results for $6p5d\ ^1D_2$ and $6p5d\ ^3D_2$ levels has nothing to do with differences in the structure models but comes from the difference in the scattering calculations. In a first order theory, like UFOMBT, in nonrelativistic approximation the excitation of both $6p5d\ ^1D_2$ and $6p5d\ ^3D_2$ levels from the $6s^2\ ^1S$ ground state can occur by exchange scattering only. As incident electron energy increases, the exchange scattering decreases which leads to very small values of the excitation cross section. Account of relativistic corrections in UFOMBT does not change this situation because the singlet-triplet mixing in the ground state is negligible, while the singlet-triplet mixing for $6p5d\ ^1D_2$ and $6p5d\ ^3D_2$ levels brings contributions from exchange transitions only. On other hand, in a close-coupling theory excitation of $6p5d\ ^1D_2$ level (in non-relativistic approximation) can occur as a two- (or more) step processes. Such processes, for example $6s^2\ ^1S \rightarrow 6s5d\ ^1D_2 \rightarrow 6p5d\ ^1D_2$, can occur via direct scattering, which leads to significantly larger cross sections. The account of relativistic corrections for the $6p5d\ ^3D_2$ level leads to significant increase of the cross section due to admixture of the singlet $6p5d\ ^1D_2$ level, see Eq. (5i).

C. Ionization

Total ionization ($Q^+ + Q^{++} + \dots = Q_i$) and single ionization (Q^+) cross sections were measured by Dettmann and Karstensen [17] and total ionization (Q_i) by Vainshtein *et al.* [18]. The CCC results are available only for Q^+ (threshold for double ionization is at 15.2 eV). These results are shown in Fig. 22. It is clear that the CCC method substantially underestimates the experimental Q^+ . At incident electron energies above 15 eV this is related to the opening of the $5p^6$ shell. This process is not accounted for in the CCC model (which has

inert inner shells). However, below the inner shells ionization threshold the CCC method should be able to account for all major ionization channels. Inclusion in the CCC calculations G-states and other states with larger angular momentum will result in a larger ionization cross section. The convergence in the TICS, with increasing target-space orbital angular momentum, is relatively fast [36] and we estimate that CCC results should converge to values 10%-15% larger than the present results. This correction of the CCC results would bring them in a very good agreement with measurements of TICS by Vainshtein *et al.* [18] in the region of the first TICS maximum. The discrepancy between the experimental results and between the experimental and the theoretical results in this energy range makes it impossible for us to present a reliable set of recommended TICS values. More accurate theoretical calculations or/and new independent measurements are required to draw any definite conclusions. For the time being, we arbitrarily renormalized the results of Dettmann and Karstensen [17] at the first maximum to the value of $13\text{e-}16\text{ cm}^2$. These renormalized values are listed in Table VII.

D. Elastic scattering, momentum transfer and total scattering

Elastic scattering and momentum transfer cross sections are available from a number of calculations. They are shown in Figs. 23 and 24, respectively. Our recommended values are given in Table VIII, where we have also included the recommended total electron scattering cross sections, see Fig. 25, based mainly on the CCC results. At low energies, the experimental results of Romanyuk *et al.* [19] are in poor agreement with our results as well as with the results of all other calculations. Hence we suppose that the present theoretical results are more accurate than the experimental ones.

IV. CONCLUSIONS

We have presented a recommended set of integrated cross sections for electron scattering by the ground state of barium. For most of the transitions presented here no previous

experimental or theoretical data are available. We expect our results to be useful in practical applications and will stimulate further experimental and theoretical effort to further improve the cross section data set.

ACKNOWLEDGMENTS

We are grateful to V.Kelemen and A.Stauffer for communicating their data in electronic form. Support of the Australian Research Council and the Flinders University of South Australia, the National Science Foundation, and the National Aeronautic and Space Administration is acknowledged. We are also indebted to the South Australian Centre for High Performance Computing and Communications. The work at the Los Alamos National Laboratory has been performed under the auspices of the US Department of Energy and has been partially supported by the Electric Power Research Institute.

REFERENCES

- [1] R. P. Mildren, D. J. W. Brown, R. J. Carman, and J. A. Piper, *Optics Communications* **120**, 112 (1995).
- [2] R. P. Mildren, D. J. W. Brown, and J. A. Piper, *IEEE Journal of Quantum Electronics* **33**, 1717 (1997).
- [3] R. P. Mildren, D. J. W. Brown, and J. A. Piper, *J. Appl. Phys.* **82**, 2039 (1997).
- [4] R. P. Mildren, D. J. W. Brown, and J. A. Piper, *Optics Communication* **137**, 299 (1997).
- [5] A. K. Bhattacharya, *J. Appl. Phys.* **137**, 299 (1997).
- [6] C. M. Yang and A. E. Rodrigez, Wright Laboratory, Report TR-92-006, Wright Patterson AFB, Ohio, March 1992.
- [7] E. M. Wescott, H. C. Stenbaek-Nielsen, J. J. Hallinan, C. S. Deehr, G. J. Romick, S. V. Olson, J. G. Roederer, and R. Sydora, *Geophys. Res. Lett.* **7**, 1037 (1980).
- [8] D. J. Simons, M. B. Pongratz, G. M. Smith, and G. E. Barasch, *J. Geophys. Res.* **86**, 1576 (1981).
- [9] D. Winske, *J. Geophys. Res.* **93**, 2539 (1988).
- [10] S. C. Chapman, *J. Geophys. Res.* **94**, 227 (1989).
- [11] R. W. Shuk and E. P. Szusgzewiez, *J. Geophys. Res.* **96**, 1337 (1991).
- [12] E. M. Wescott *et al.*, *J. Geophys. Res.* **98**, 3711 (1993).
- [13] S. T. Chen and A. Gallagher, *Phys. Rev. A* **14**, 593 (1976).
- [14] S. Trajmar and J. C. Nickel, *Adv. Atom. Mol. Phys.* **30**, 45 (1992).
- [15] S. Jensen, D. Register, and S. Trajmar, *J. Phys. B* **11**, 2367 (1978).
- [16] S. Wang, S. Trajmar, and P. W. Zetner, *J. Phys. B* **27**, 1613 (1994).

- [17] J. Dettmann and F. Karstensen, *J. Phys. B* **15**, 287 (1982).
- [18] L. A. Vainshtein, V. I. Ochcur, V. I. Rakhovskii, and A. M. Stepanov, *Sov. Phys. -JETP* **34**, 271 (1972).
- [19] N. I. Romanyuk, O. B. Shpenik, and I. P. Zapesochny, *JETP Lett.* **32**, 452 (1980).
- [20] D. Gregory and M. Fink, *Atom. Data Nucl. Data Tables* **14**, 39 (1974).
- [21] I. I. Fabrikant, *J. Phys. B* **13**, 603 (1980).
- [22] J. Yuan and Z. Zhang, *Phys. Rev. A* **42**, 5363 (1990).
- [23] J. Yuan and Z. Zhang, *Phys. Lett. A* **168**, 291 (1992).
- [24] R. Szmytkowski and J. E. Sienkiewicz, *Phys. Rev. A* **50**, 4007 (1994).
- [25] V. I. Kelemen, E. Y. Remeta, and E. P. Sabad, *J. Phys. B* **28**, 1527 (1995).
- [26] G. F. Gribakin, B. V. Gul'tsev, V. K. Ivanov, M. Y. Kuchiev, and A. R. Tancic, *Phys. Lett. A* **164**, 73 (1992).
- [27] R. E. Clark, J. Abdallah Jr., G. Csanak, and S. P. Kramer, *Phys. Rev. A* **40**, 2935 (1989).
- [28] R. Srivastava, T. Zuo, R. P. McEachran, and A. D. Stauffer, *J. Phys. B* **25**, 3709 (1992).
- [29] R. Srivastava, R. P. McEachran, and A. D. Stauffer, *J. Phys. B* **25**, 4033 (1992).
- [30] D. V. Fursa and I. Bray, *Phys. Rev. A* **57**, R3150 (1998).
- [31] D. V. Fursa and I. Bray, *Phys. Rev. A* **59**, 282 (1999).
- [32] D. V. Fursa and I. Bray, *J. Phys. B* **30**, 5895 (1997).
- [33] H. E. Saraph, *Comp. Phys. Comm.* **3**, 256 (1972).
- [34] P. W. Zetner, S. Trajmar, S. Wang, I. Kanik, G. Csanak, R. E. Clark, J. Abdallah, and J. C. Nickel, *J. Phys. B* **30**, 5317 (1997).

- [35] C. W. Bauschlicher Jr, R. L. Jaffe, S. R. Langhoff, F. G. Mascarello, and H. Partridge, *J. Phys. B* **18**, 2147 (1985).
- [36] I. Bray, *Phys. Rev. Lett.* **73**, 1088 (1994).
- [37] C. E. Moore, *Atomic Energy Levels, Circ. No. 467 Vol. III* (Natl. Bur. Stand. (U.S.), U.S. GPO, Washington, DC, 1949).
- [38] H. P. Palenius, *Phys. Lett.* **56A**, 451 (1976).

TABLES

TABLE I. Excitation energies and dominant configurations for the barium levels from CCC and CC(55) non-relativistic calculations. The experimental data are from Refs. [37] and [38] ($5d^2$ 1S level). States are labeled by the major configuration.

experiment		present		
label	E(eV)	label	E(eV)	Dominant configurations
$6s^2$ 1S	0.00	$6s^2$	0.00	$0.944(6s^2$ $^1S) + 0.228(6p^2$ $^1S) - 0.191(7s6s$ $^1S)$
$5d^2$ 1S	3.32	$5d^2$	3.34	$0.591(7s6s$ $^1S) - 0.519(5d^2$ $^1S) + 0.369(nd5d$ $^1S)$
$6s6p$ 1P	2.24	$6s6p$	2.27	$0.800(6p6s$ $^1P) - 0.504(5d6p$ $^1P) - 0.256(7p6s$ $^1P)$
$6s7p$ 1P	3.54	$6s7p$	3.62	$0.688(7p6s$ $^1P) - 0.550(5d6p$ $^1P) + 0.331(5d7p$ $^1P)$
$6s8p$ 1P	4.04	$6s8p$	4.14	$0.788(6snp$ $^1P) + 0.301(5d6p$ $^1P) - 0.505(5d7p$ $^1P)$
$6s5d$ 1D	1.41	$6s5d$	1.44	$0.896(5d6s$ $^1D) - 0.226(5d7s$ $^1D) - 0.226(5d^2$ $^1D)$
$5d^2$ 1D	2.86	$5d^2$	3.04	$0.798(5d^2$ $^1D) - 0.442(nd5d$ $^1D) + 0.350(6p^2$ $^1D)$
$6s6d$ 1D	3.75	$6s6d$	3.79	$0.893(nd6s$ $^1D) - 0.369(5d7s$ $^1D) - 0.162(6p^2$ $^1D)$
$5d6p$ 1D	2.86	$5d6p$	2.87	$0.946(5d6p$ $^1D) - 0.289(5d7p$ $^1D)$
$5d6p$ 1F	3.32	$5d6p$	3.35	$0.852(5d6p$ $^1F) - 0.424(5d7p$ $^1F) + 0.280(nf6s$ $^1F)$
$6s4f$ 1F	4.31	$6s4f$	4.36	$0.973(nf6s$ $^1F) + 0.165(5d7p$ $^1F) - 0.141(nd6p$ $^1F)$
$6s6p$ 3P	1.62	$6s6p$	1.59	$0.960(6p6s$ $^3P) - 0.161(5d6p$ $^3P) - 0.116(6p7s$ $^3P)$
$5d6p$ 3P	3.20	$5d6p$	3.30	$0.873(5d6p$ $^3P) - 0.394(5d7p$ $^3D) - 0.215(7p6s$ $^3P)$
$5d^2$ 3P	2.94	$5d^2$	3.11	$0.799(5d^2$ $^3P) + 0.458(nd5d$ $^3D) + 0.389(6p^2$ $^3P)$
$6s5d$ 3D	1.16	$6s5d$	1.21	$0.955(5d6s$ $^3D) - 0.201(5d7s$ $^3D) - 0.112(nf6p$ $^3D)$
$6s6d$ 3D	3.85	$6s6d$	3.82	$0.961(nd6s$ $^3D) - 0.208(5d7s$ $^3D)$
$5d6p$ 3D	3.06	$5d6p$	3.12	$0.924(5d6p$ $^3D) - 0.361(5d7p$ $^3D)$
$5d6p$ 3F	2.86	$5d6p$	2.88	$0.934(5d6p$ $^3F) - 0.289(5d7p$ $^3F) + 0.129(nf6s$ $^3F)$

TABLE II. Recommended values for $Q_{app}(6s6p^1P_1)$, $Q_{cascade}(6s6p^1P_1)$, and $Q(6s6p^1P_1)$ in units of 10^{-16} cm^2 .

E_0 (eV)	$Q_{App}(6s6p^1P_1)$	$Q_{cascade}/Q_{App}$ (%)	$Q_{cascade}(6s6p^1P_1)$	$Q(6s6p^1P_1)$
2.50	4.56	0.00	0.00	4.56
3.00	12.00	0.00	0.00	12.00
4.00	25.84	15.54	4.02	21.83
5.00	33.34	17.71	5.90	27.43
6.00	37.26	19.52	7.27	29.98
7.00	39.89	20.61	8.22	31.67
8.35	39.00	19.80	7.72	31.28
9.00	40.44	17.53	7.09	33.35
10.00	41.24	15.63	6.45	34.79
11.44	42.56	13.48	5.74	36.82
15.00	42.47	15.23	6.47	36.00
20.00	39.78	13.14	5.23	34.55
30.00	35.01	11.19	3.92	31.09
36.67	32.39	10.38	3.36	29.03
41.44	30.78	9.94	3.06	27.72
50.00	28.11	9.57	2.69	25.42
60.00	25.49	9.15	2.33	23.16
80.00	21.55	8.30	1.79	19.76
100.00	18.75	7.44	1.40	17.35
200.00	11.65	6.56	0.76	10.88
400.00	6.81	5.46	0.37	6.44
600.00	4.92	5.17	0.25	4.66
897.60	3.52	4.91	0.17	3.35

TABLE III. Recommended $Q(6s7p^1P_1)$, $Q_{app}(6s7p^1P_1)$, $Q(6s8p^1P_1)$, and $Q_{app}(6s8p^1P_1)$ values in units of 10^{-16} cm^2 .

E_0 (eV)	$Q(6s7p^1P_1)$	$Q_{App}(6s7p^1P_1)$	$Q(6s8p^1P_1)$	$Q_{App}(6s8p^1P_1)$
5.00	0.48	0.70	0.22	0.27
6.00	0.76	1.04	0.45	0.53
7.00	0.73	1.06	0.71	0.81
8.35	0.81	1.20	0.78	0.90
9.00	0.49	0.86	0.64	0.76
10.00	0.35	0.70	0.69	0.80
11.44	0.33	0.60	1.00	1.08
15.00	0.32	0.65	1.18	1.30
20.00	0.39	0.67	1.30	1.40
30.00	0.47	0.71	1.45	1.54
36.67	0.50	0.72	1.46	1.54
50.00	0.50	0.70	1.49	1.55
60.00	0.49	0.65	1.45	1.50
80.00	0.46	0.58	1.25	1.35
100.00	0.42	0.54	1.10	1.14
200.00	0.30	0.37	0.74	0.77
400.00	0.19	0.23	0.44	0.45
600.00	0.14	0.17	0.31	0.32
897.60	0.10	0.12	0.23	0.23

TABLE IV. Recommended $Q(5d^2\ ^1S_0)$, $Q(6s5d^1D_2)$, $Q(5d^2\ ^1D_2)$, and $Q(6s6d^1D_2)$ values in units of 10^{-16} cm^2 .

E_0 (eV)	$Q(5d^2\ ^1S_0)$	$Q(6s5d^1D_2)$	$Q(5d^2\ ^1D_2)$	$Q(6s6d^1D_2)$
5.00	0.81	5.45	2.74	1.21
6.00	0.89	4.95	2.54	1.79
7.00	1.23	4.07	2.41	2.25
8.35	1.79	3.69	1.87	2.21
9.00	1.17	3.59	1.57	1.96
10.00	0.70	3.53	1.51	2.01
11.44	0.55	3.39	1.44	2.28
15.00	0.48	2.99	1.28	2.13
20.00	0.36	2.74	0.90	1.89
30.00	0.38	2.46	0.51	1.50
36.67	0.38	2.33	0.37	1.29
41.44	0.38	2.24	0.31	1.15
50.00	0.35	2.00	0.24	0.97
60.00	0.31	1.78	0.19	0.81
80.00	0.27	1.44	0.13	0.62
100.00	0.23	1.22	0.10	0.50
200.00	0.14	0.69	0.043	0.25
400.00	0.08	0.37	0.018	0.125
600.00	0.05	0.25	0.012	0.083
897.60	0.03	0.16	0.008	0.056

TABLE V. Recommended $Q(6p5d^1D_2)$, $Q(6p5d^1F_3)$, $Q(6s4f^1F_3)$, and $Q(6p5d^3D_2)$ values in units of 10^{-16} cm^2 .

E_0 (eV)	$Q(6p5d^1D_2)$	$Q(6p5d^1F_3)$	$Q(6s4f^1F_3)$	$Q(6p5d^3D_2)$
5.00	0.446	0.826	0.249	0.150
6.00	0.456	0.661	0.297	0.098
7.00	0.376	0.506	0.580	0.093
8.35	0.355	0.424	0.626	0.045
9.00	0.319	0.345	0.617	0.053
10.00	0.249	0.322	0.718	0.026
11.44	0.246	0.344	0.661	0.024
15.00	0.256	0.320	0.571	0.010
20.00	0.238	0.287	0.457	0.005
30.00	0.161	0.231	0.314	0.0025
36.67	0.127	0.195	0.252	0.0019
41.44	0.105	0.177	0.221	0.0013
50.00	0.079	0.148	0.181	0.00098
60.00	0.060	0.128	0.147	0.00068
80.00	0.037	0.099	0.106	0.00039
100.00	0.026	0.081	0.082	0.00025
200.00	0.0072	0.041	0.04	-
400.00	0.0009	0.022	0.019	-
600.00	0.00025	0.015	0.012	-
897.60	0.00017	0.0097	0.0083	-

TABLE VI. Recommended $Q(6s6p^3P_J)$ and $Q(6s5d^3D_J)$ values in units of 10^{-16} cm^2 .

E_0 (eV)	$Q(6s6p^3P_J)$			$Q(6s5d^3D_J)$		
	J=0	J=1	J=2	J=1	J=2	J=3
5.00	0.133	0.553	0.664	1.232	2.130	2.875
6.00	0.093	0.451	0.463	0.983	1.712	2.293
7.00	0.092	0.460	0.461	0.710	1.247	1.656
8.35	0.041	0.323	0.207	0.385	0.710	0.899
9.00	0.024	0.269	0.122	0.272	0.524	0.635
10.00	0.023	0.278	0.113	0.199	0.404	0.464
11.44	0.025	0.289	0.127	0.135	0.297	0.316
15.00	0.026	0.291	0.129	0.068	0.178	0.159
20.00	0.016	0.257	0.080	0.054	0.150	0.127
30.00	0.009	0.219	0.043	0.029	0.102	0.067
36.67	0.005	0.192	0.025	0.019	0.084	0.045
41.44	0.003	0.180	0.016	0.013	0.072	0.031
50.00	0.002	0.161	0.009	0.0068	0.057	0.016
60.00	0.001	0.145	0.005	0.0036	0.047	0.0084
80.00	0.0005	0.122	0.002	0.0014	0.035	0.0032
100.00	0.00024	0.107	0.0012	0.0007	0.029	0.0015
200.00	-	0.066	-	-	0.016	-
400.00	-	0.039	-	-	0.0083	-
600.00	-	0.028	-	-	0.0055	-
897.60	-	0.020	-	-	0.0037	-

TABLE VII. Estimate of ionization cross section Q_{ion} and Q^+ values in units of 10^{-16} cm^2 .

E_0 (eV)	Q_{ion}	Q^+
5.40	0.8	0.8
6.00	3.3	3.3
7.00	7.0	7.00
8.00	10.1	10.1
9.00	12.6	12.6
10.00	12.0	12.0
12.00	10.6	10.6
15.00	10.2	10.2
20.00	11.4	11.4
30.00	12.8	9.3
40.00	12.0	7.6
50.00	11.1	6.5
80.00	8.6	4.3
100.00	7.9	3.6
150.00	7.1	2.4
200.00	5.6	1.9
400.00	3.3	1.1
600.00	2.4	0.8

TABLE VIII. Recommended Q_{elas} , Q_M , and Q_{Tot} values in units of 10^{-16} cm².

E_0 (eV)	Q_{elas}	Q_M	Q_{Tot}
1.00	175.3	88.8	175.3
1.50	117.5	41.1	162.4
2.00	106.1	37.4	148.7
2.50	93.4	25.4	142.0
3.00	86.0	24.9	130.5
4.00	72.1	22.5	122.2
5.00	65.1	21.0	120.0
6.00	57.8	18.2	117.3
7.00	47.5	11.7	112.8
8.35	35.0	6.6	101.3
9.00	32.3	5.8	97.2
10.00	30.2	4.9	94.8
11.44	28.6	4.9	92.0
15.00	30.6	5.3	91.7
20.00	29.4	4.6	87.4
30.00	26.4	3.0	77.8
41.44	22.7	2.1	67.2
50.00	20.1	1.7	60.0
60.00	18.3	1.6	55.0
80.00	15.6	1.5	46.0
100.00	13.8	1.5	39.9
200.00	10.2	1.8	24.7
400.00	7.5	1.4	15.9
600.00	6.1	1.0	12.0
897.60	4.9	0.7	9.1

FIGURES

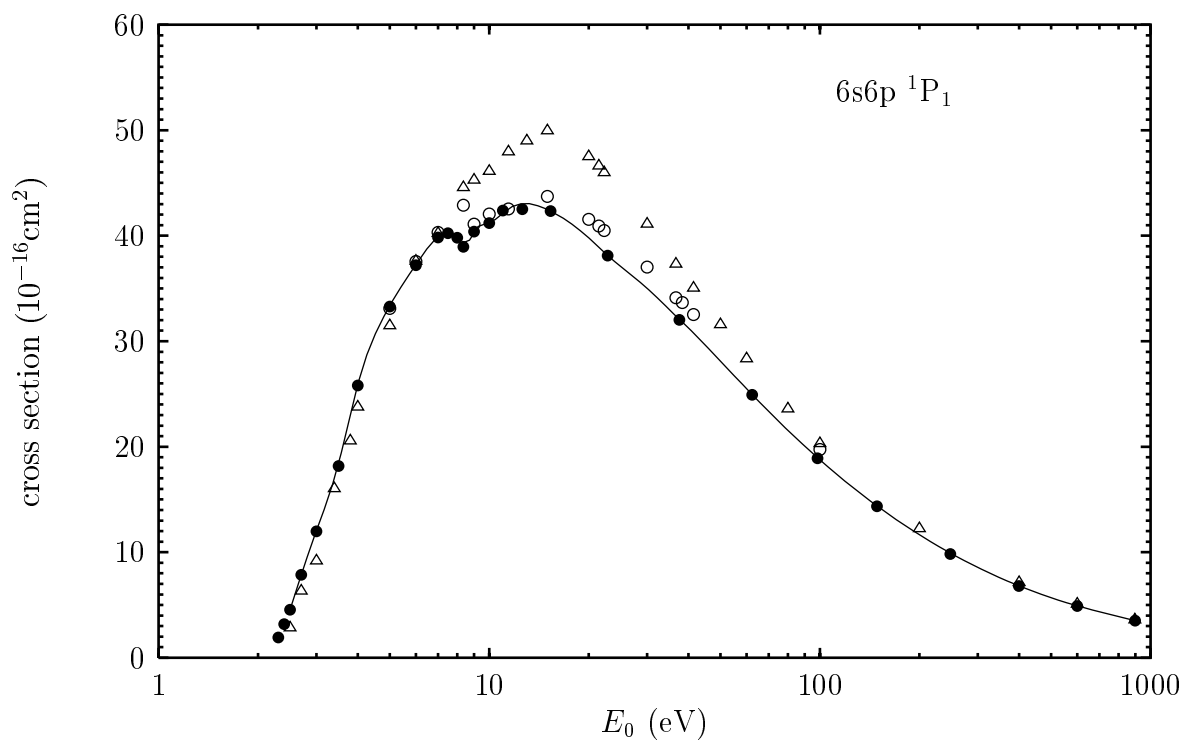


FIG. 1. Apparent $6s6p\ ^1P_1$ integral excitation cross sections: \circ , CCC; \triangle , CC(55); \bullet , Chen and Galagher [13]. The solid line represents our recommended values.

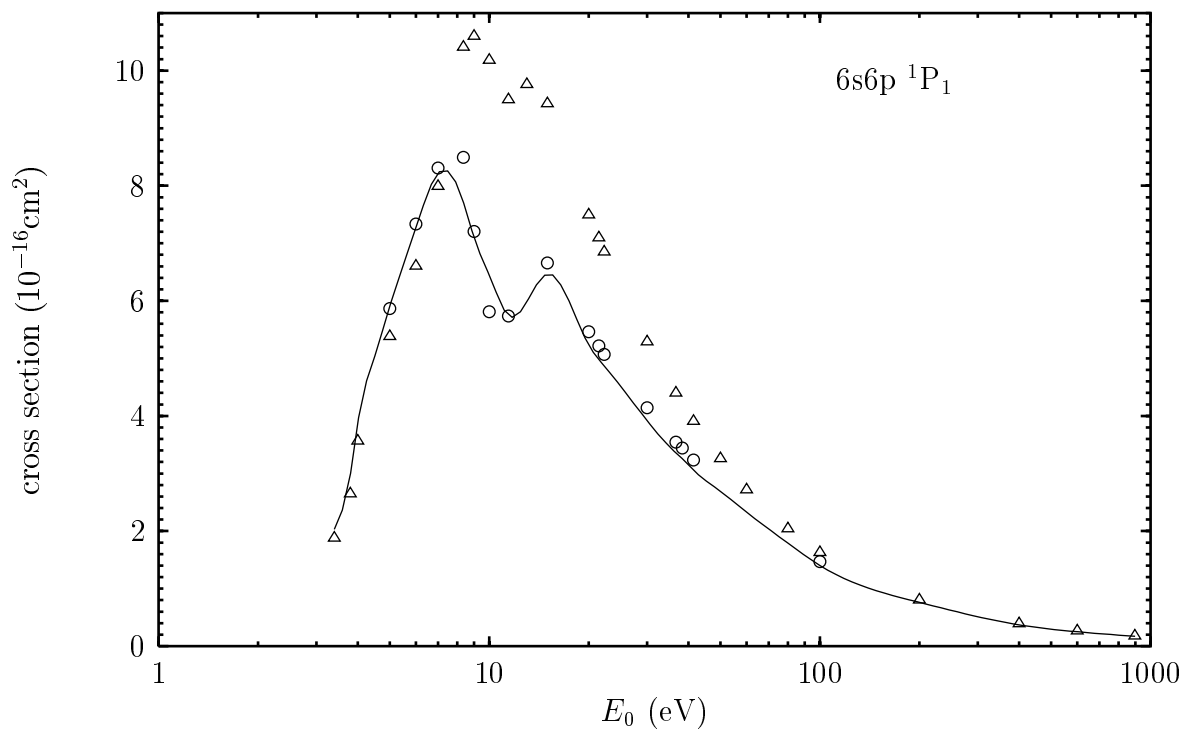


FIG. 2. Cascade contribution to the 6s6p 1P_1 level apparent excitation cross section: \circ , CCC; \triangle , CC(55). The solid line represents our recommended values.

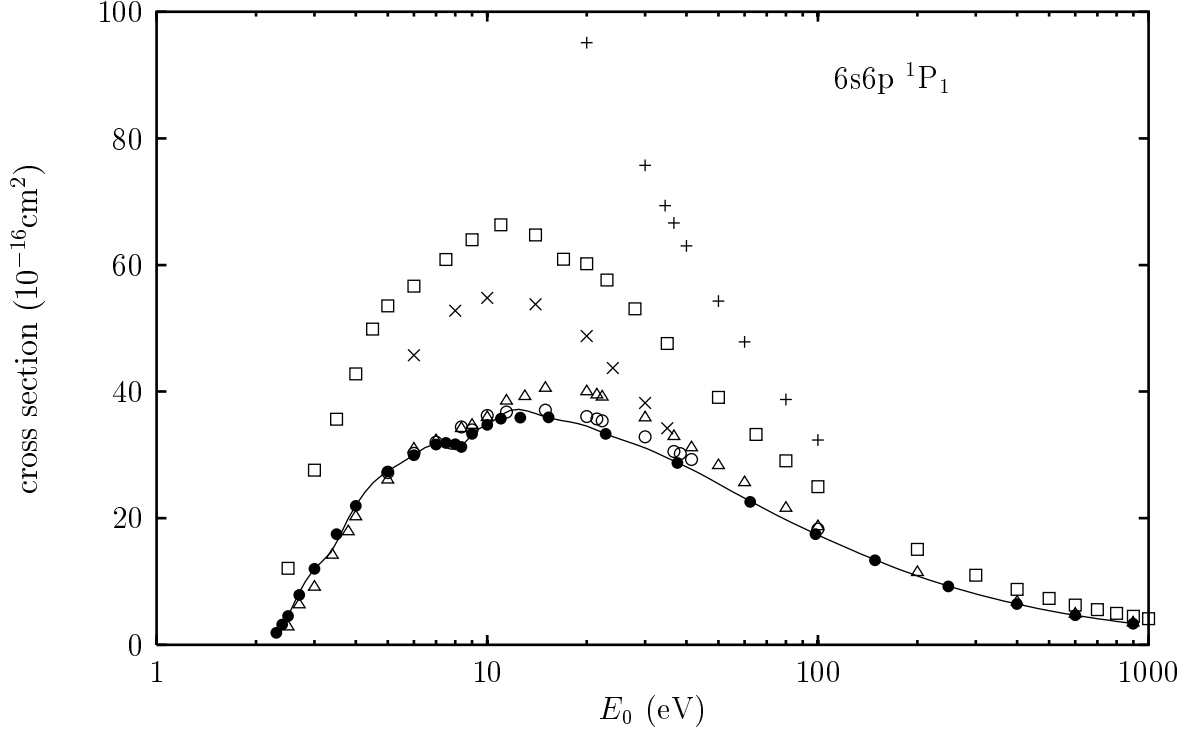


FIG. 3. Integral cross sections for excitation of the $6s6p^1P_1$ level: \circ , CCC; \triangle , CC(55); \square , UFOMBT; \times , CC(2) Fabrikant [21]; $+$, RDWA Srivastava *et al.* [28]; \bullet , obtained from apparent cross section of Chen and Gallagher [13] by subtracting theoretical (CCC and CC(55)) estimate of cascade contribution. The solid line represents our recommended values.

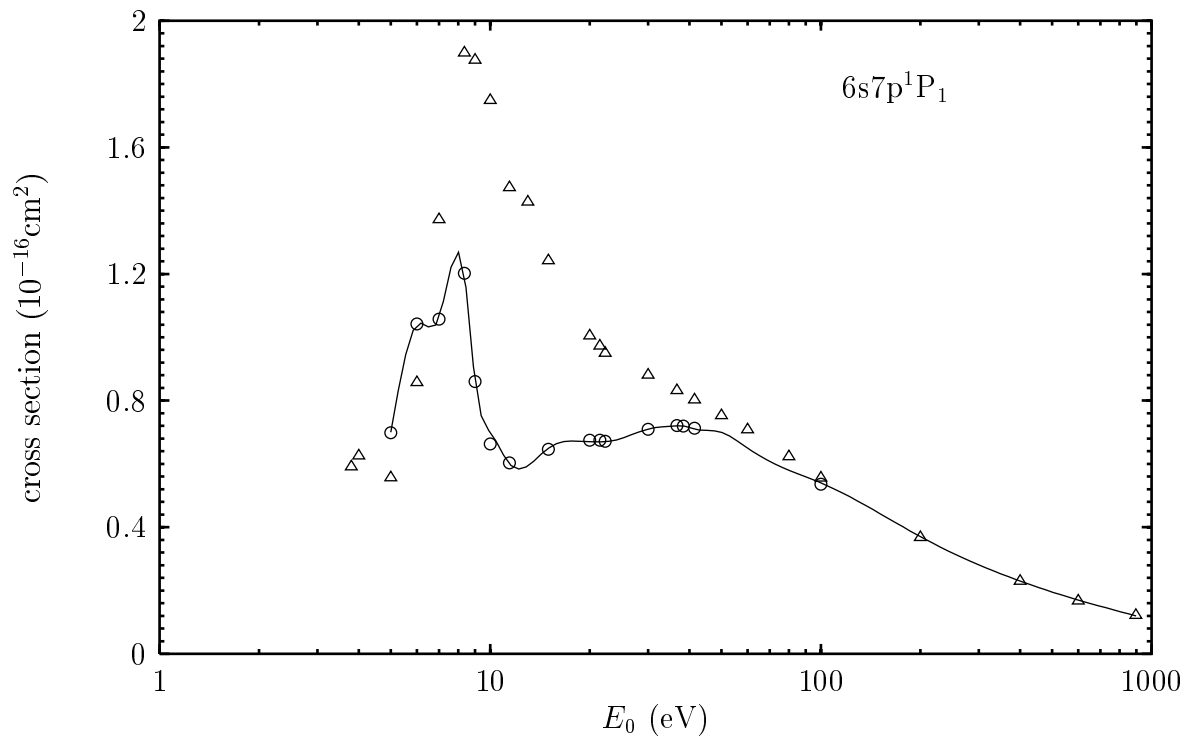


FIG. 4. Same as Fig. 1 except for the $6s7p^1P_1$ level.

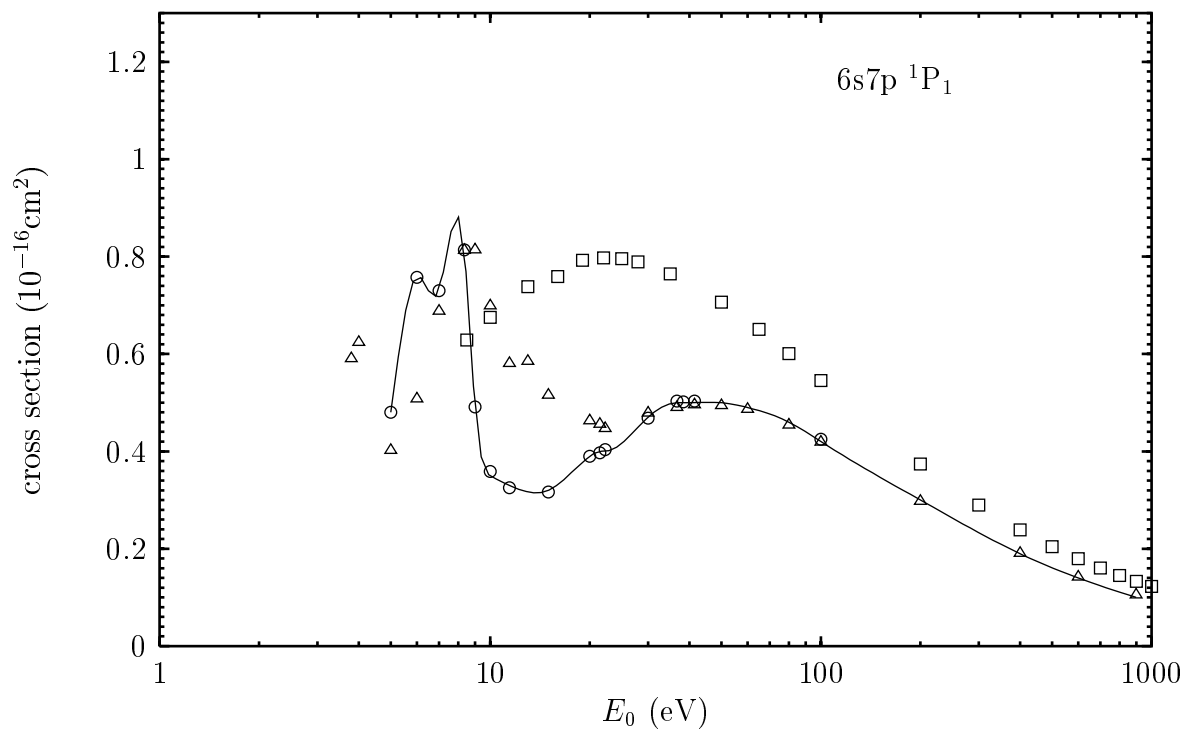


FIG. 5. Same as Fig. 3 except for the 6s7p 1P_1 level.

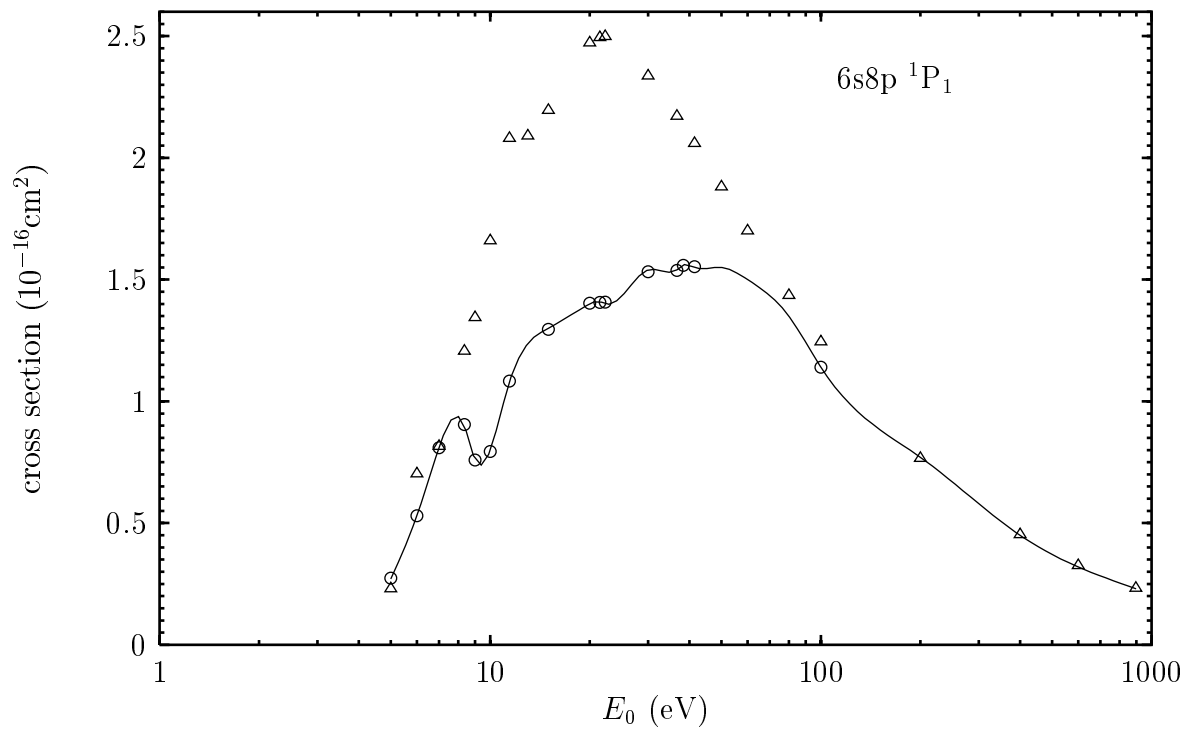


FIG. 6. Same as Fig. 1 except for the 6s8p 1P_1 level.

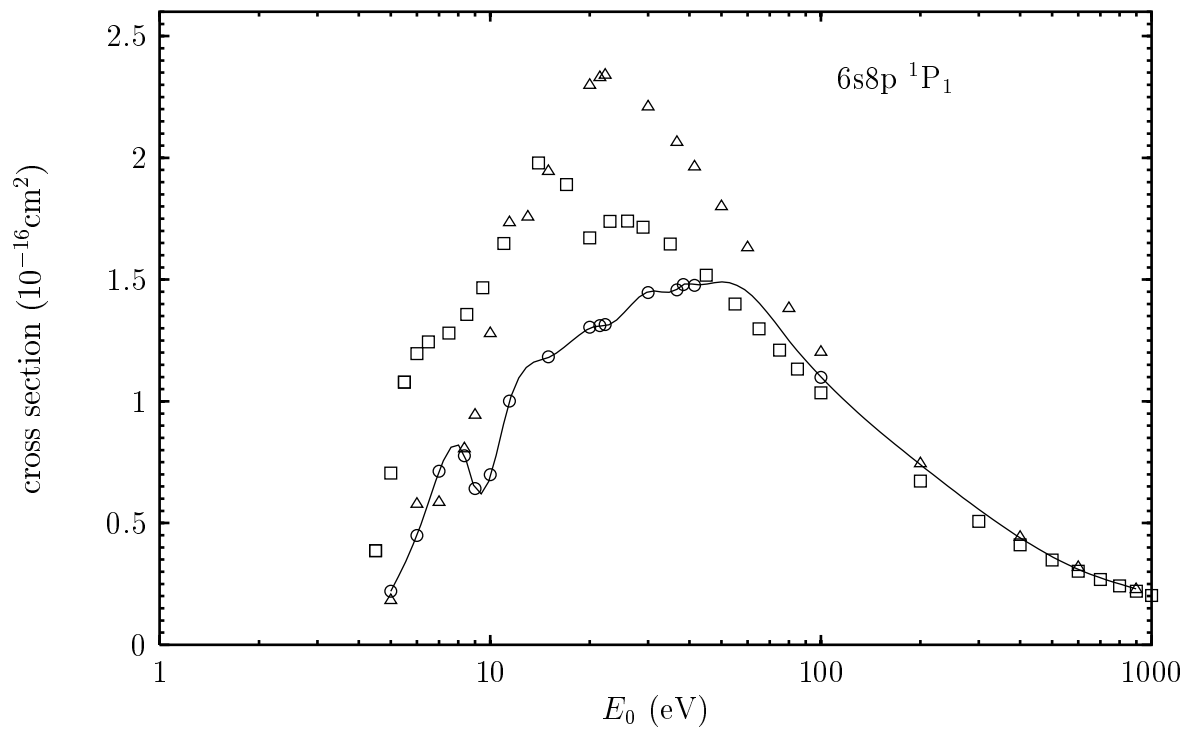


FIG. 7. Same as Fig. 3 except for the 6s8p 1P_1 level.

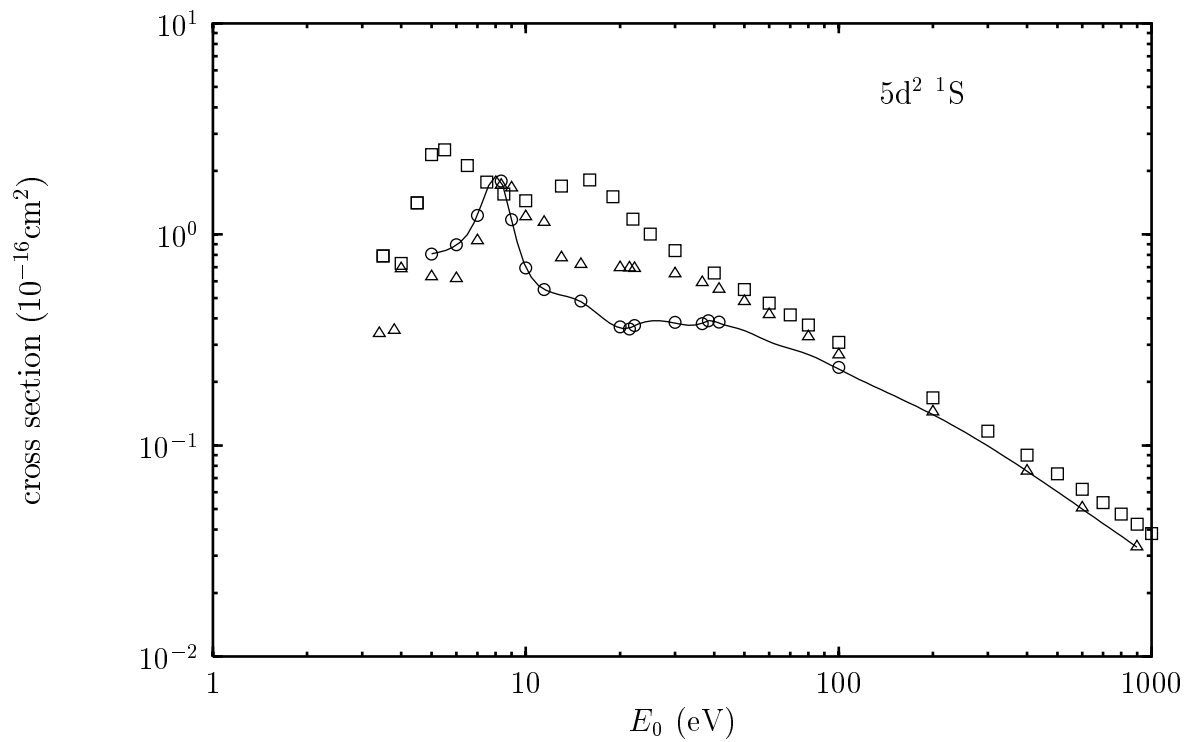


FIG. 8. Same as Fig. 3 except for the $5d^2 \ ^1S$ level.

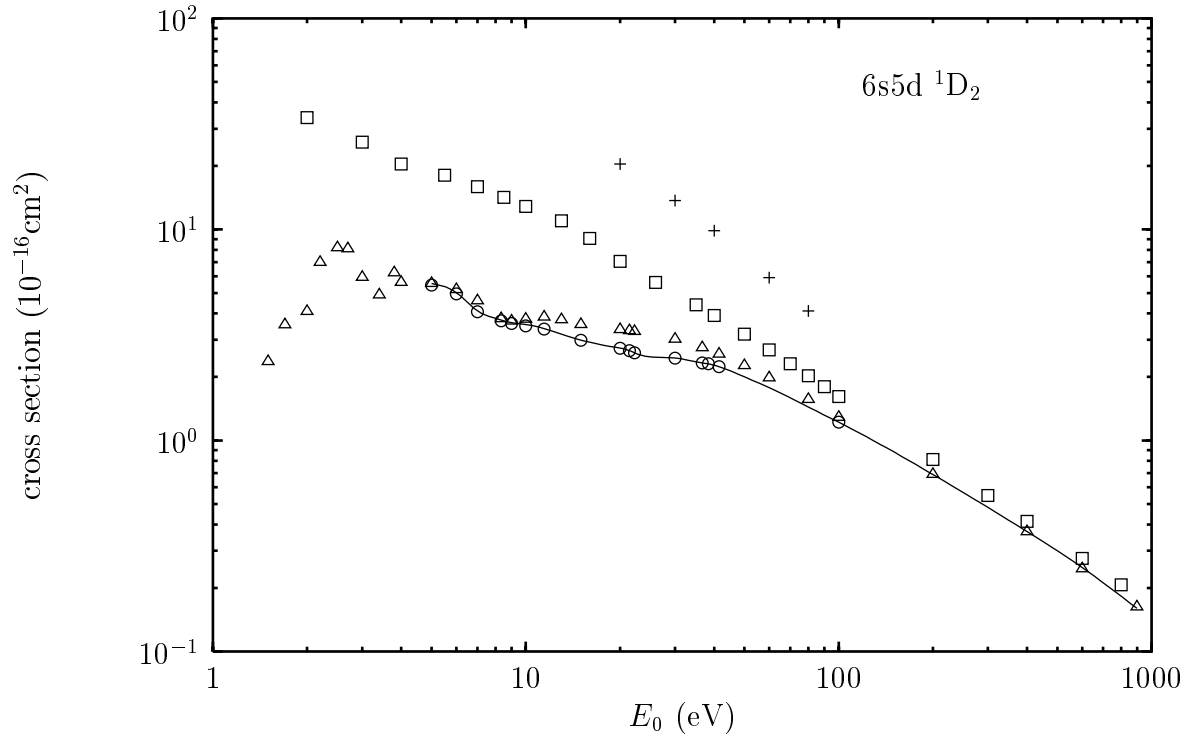


FIG. 9. Integrated cross sections for excitation of the $6s5d\ ^1D_2$ level: \circ , CCC; \triangle , CC(55); \square , UFOMBT; $+$, RDWA Srivastava *et al.* [29]. The solid line represents our recommended values.

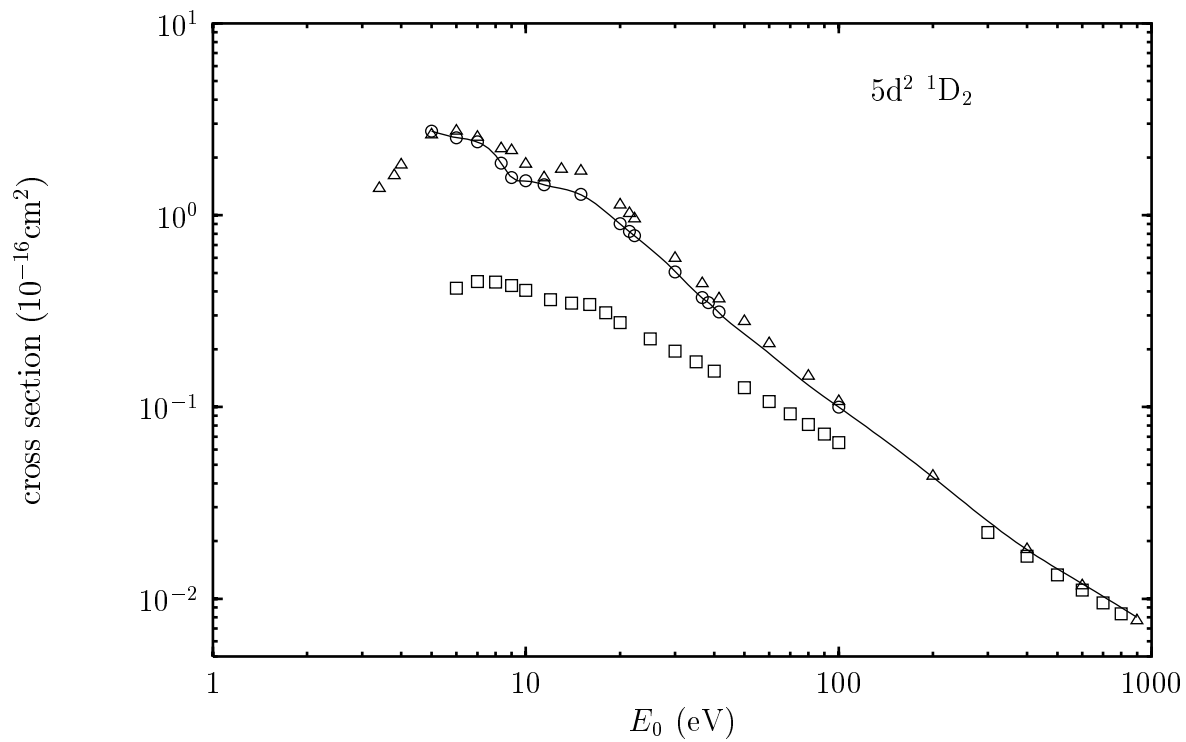


FIG. 10. Same as Fig. 9 except for the $5d^2 \ ^1D_2$ level.

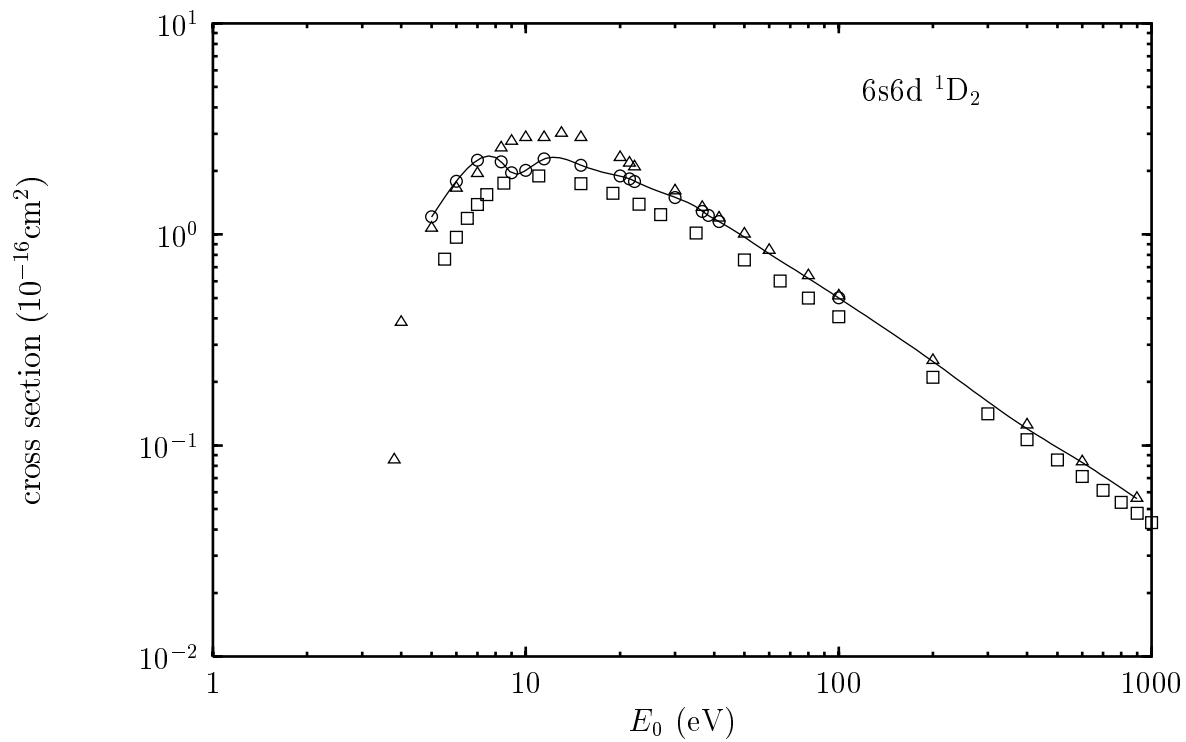


FIG. 11. Same as Fig. 9 except for the $6s6d \ ^1D_2$ level.

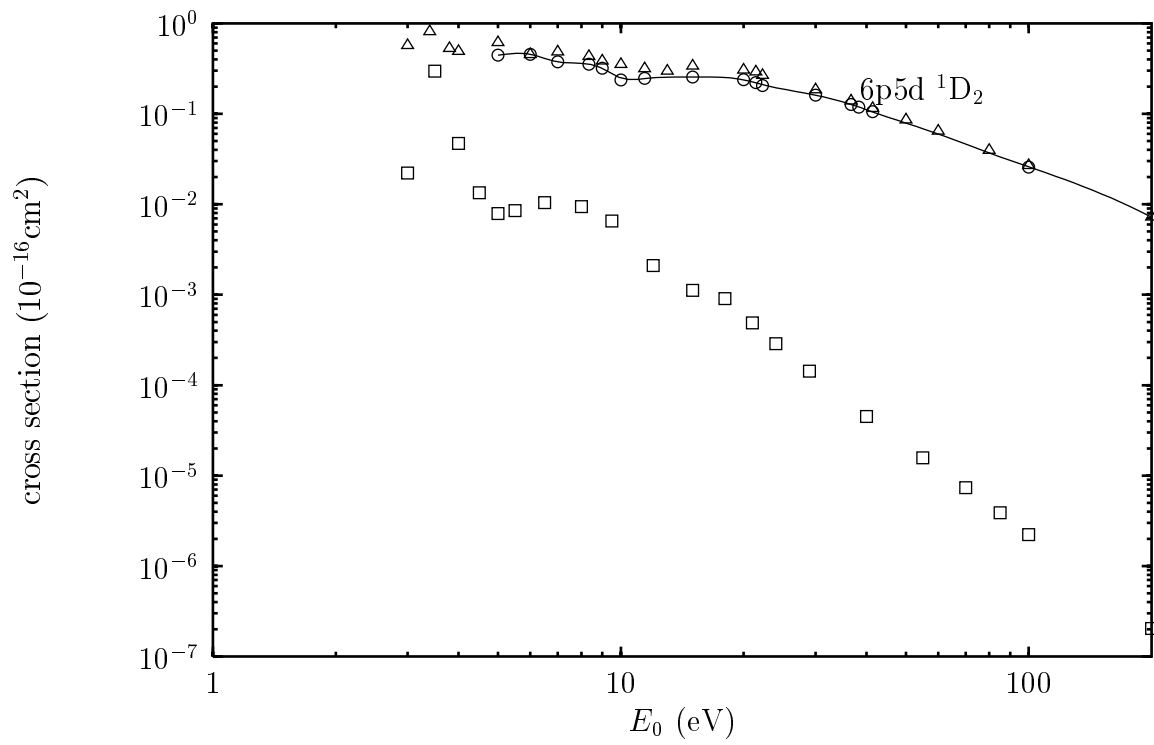


FIG. 12. Same as Fig. 9 except for the $6p5d \ ^1D_2$ level.

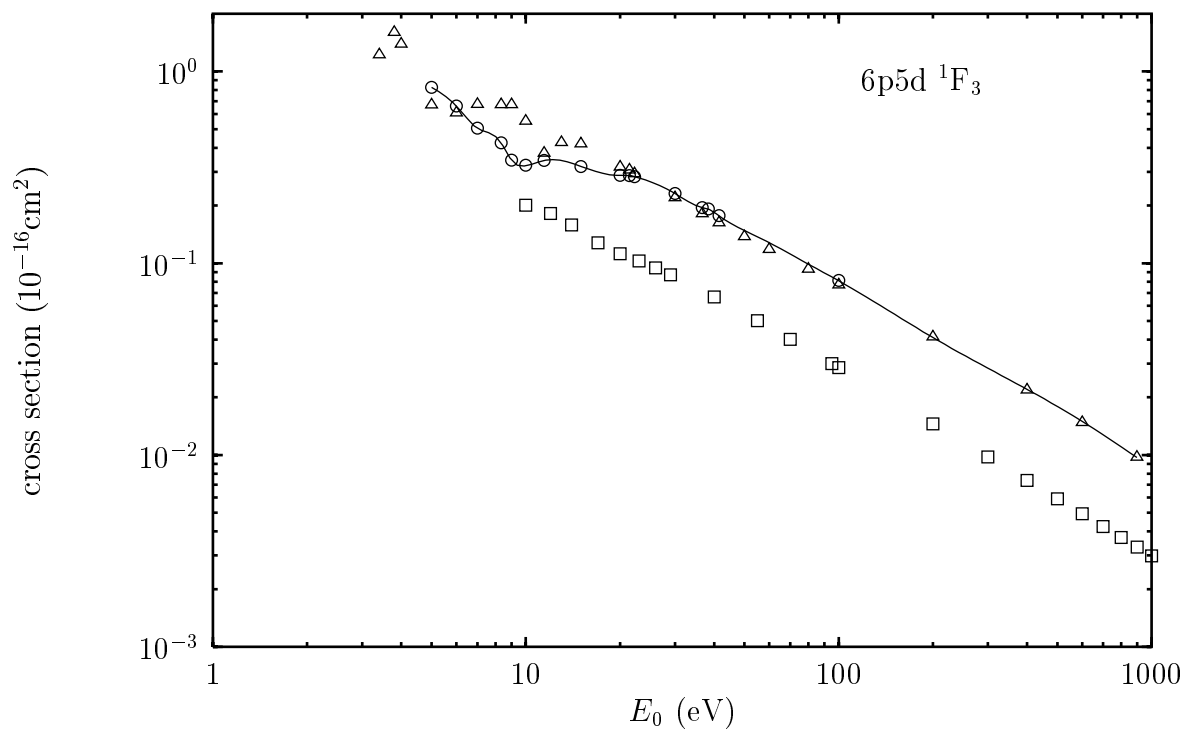


FIG. 13. Same as Fig. 9 except for the $6p5d \ ^1F_3$ level.

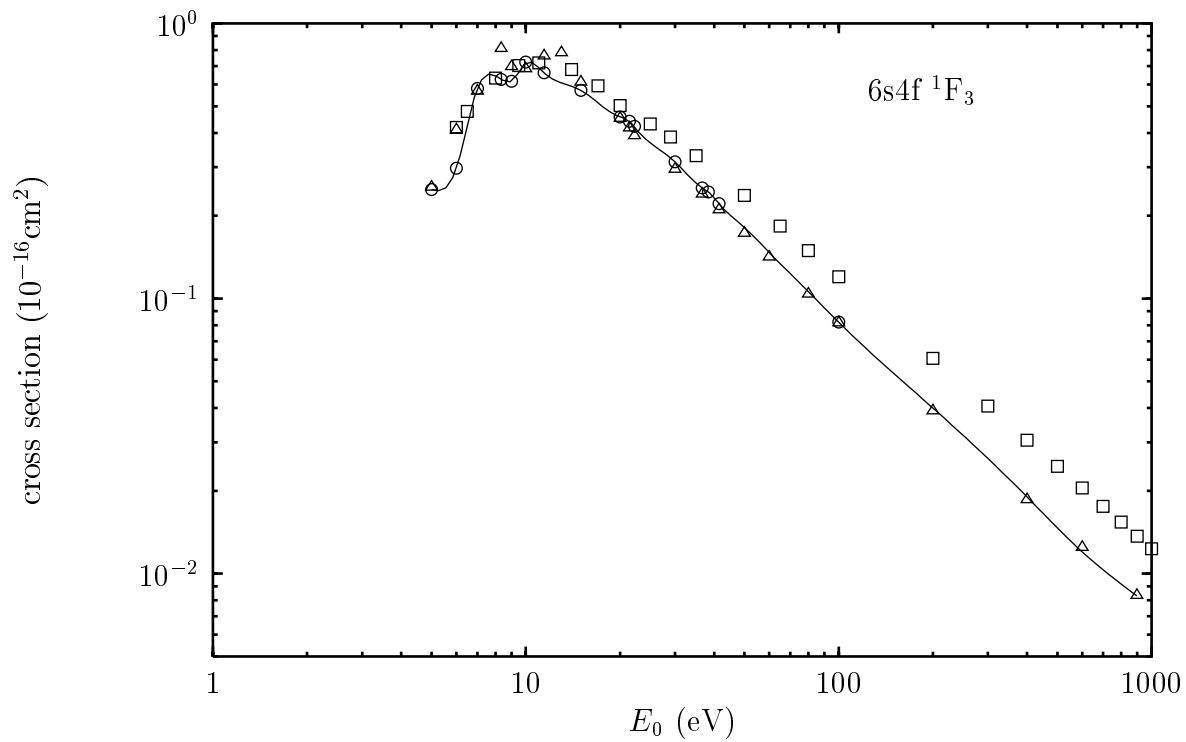


FIG. 14. Same as Fig. 9 except for the $6s4f \ ^1F_3$ level.

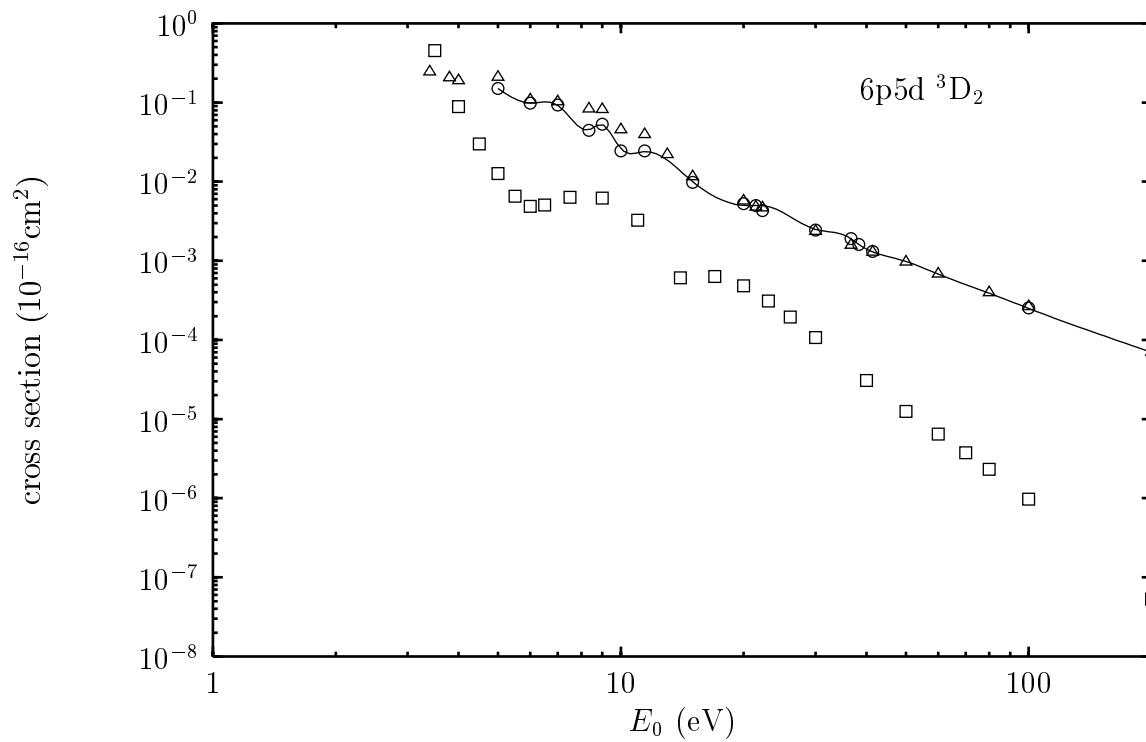


FIG. 15. Same as Fig. 9 except for the $6p5d \ ^3D_2$ level.

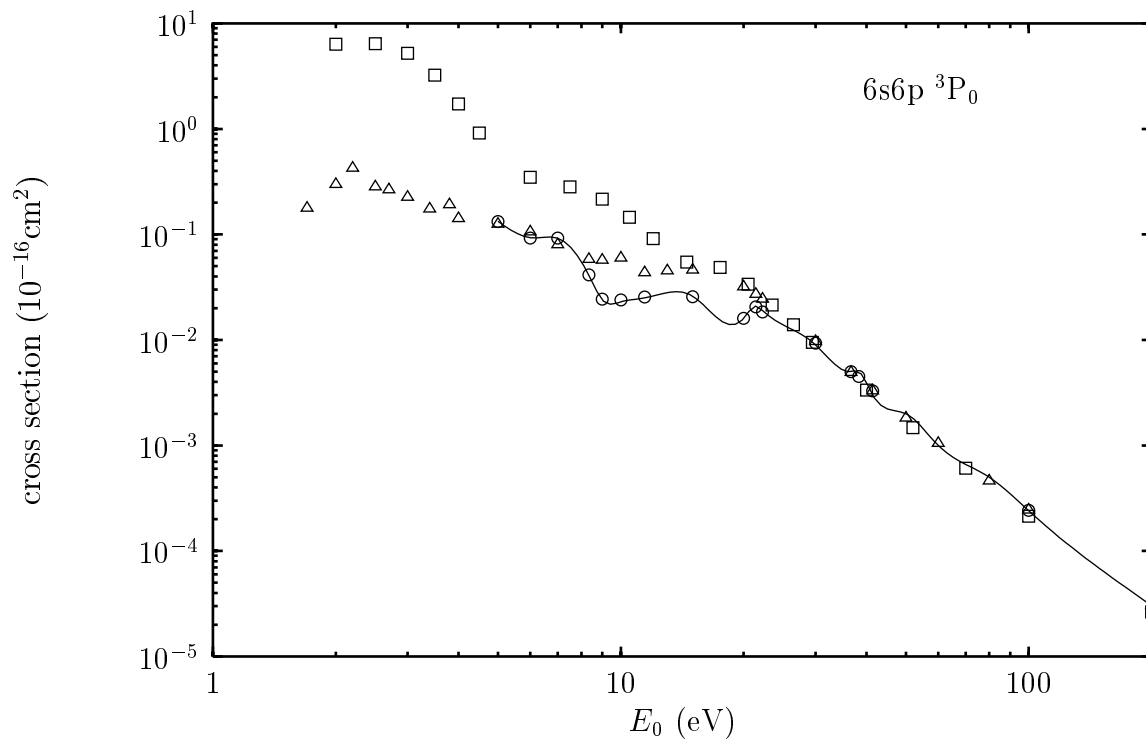


FIG. 16. Same as Fig. 9 except for the $6s6p \ ^3P_0$ level.

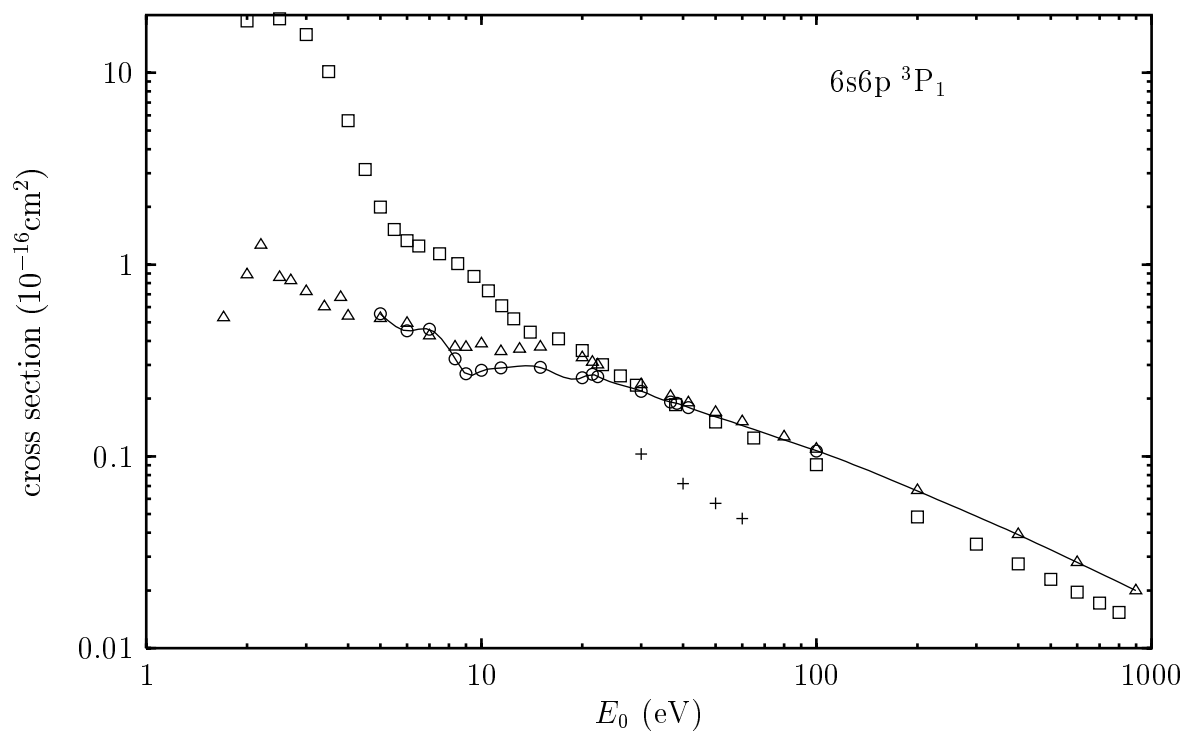


FIG. 17. Same as Fig. 9 except for the $6s6p \ ^3P_1$ level.

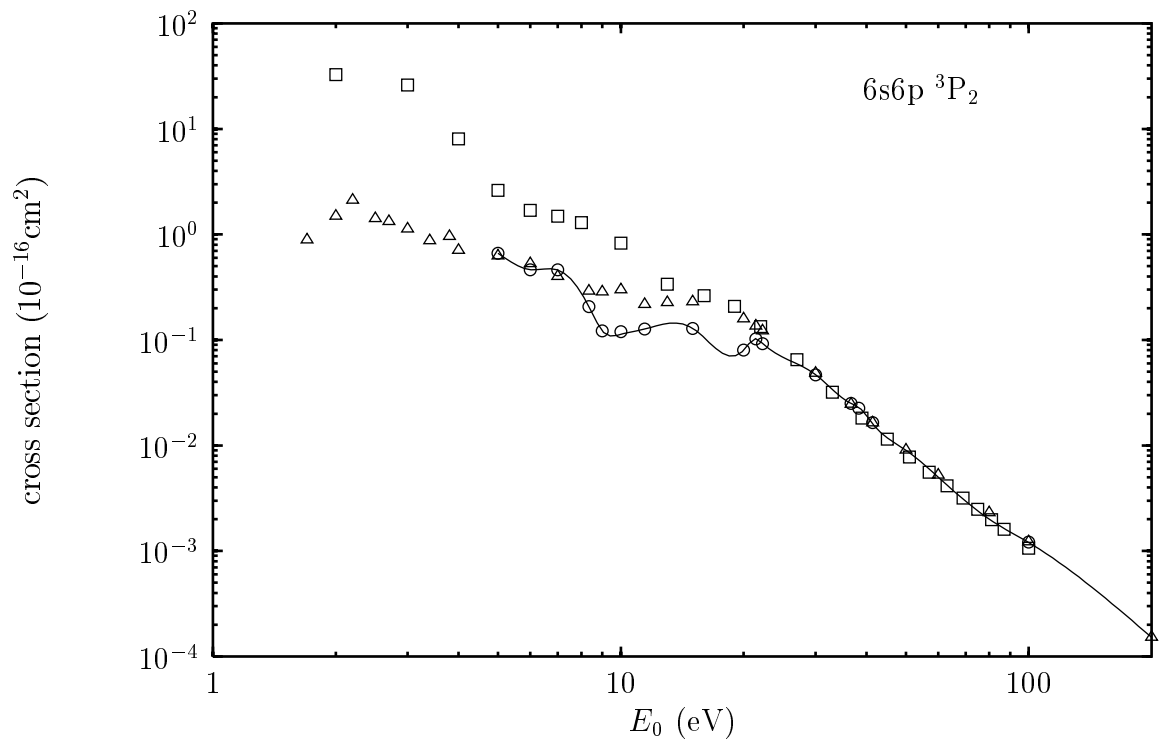


FIG. 18. Same as Fig. 9 except for the $6s6p \ ^3P_2$ level.

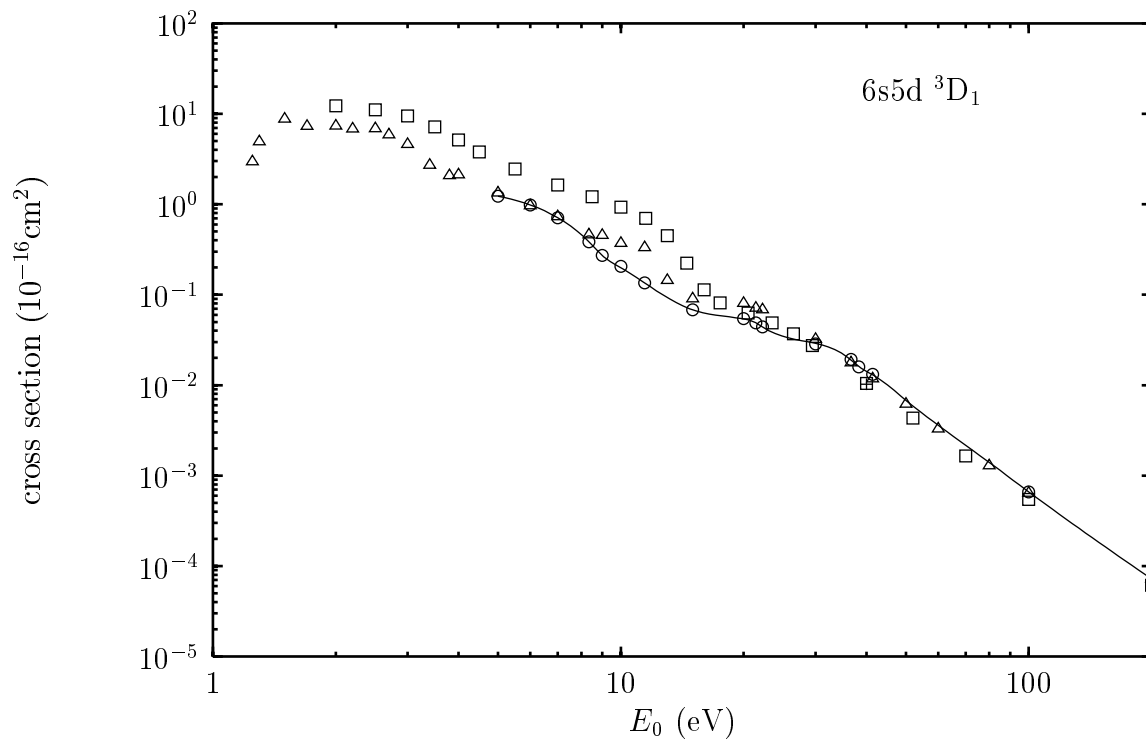


FIG. 19. Same as Fig. 9 except for the $6s5d \ ^3D_1$ level.

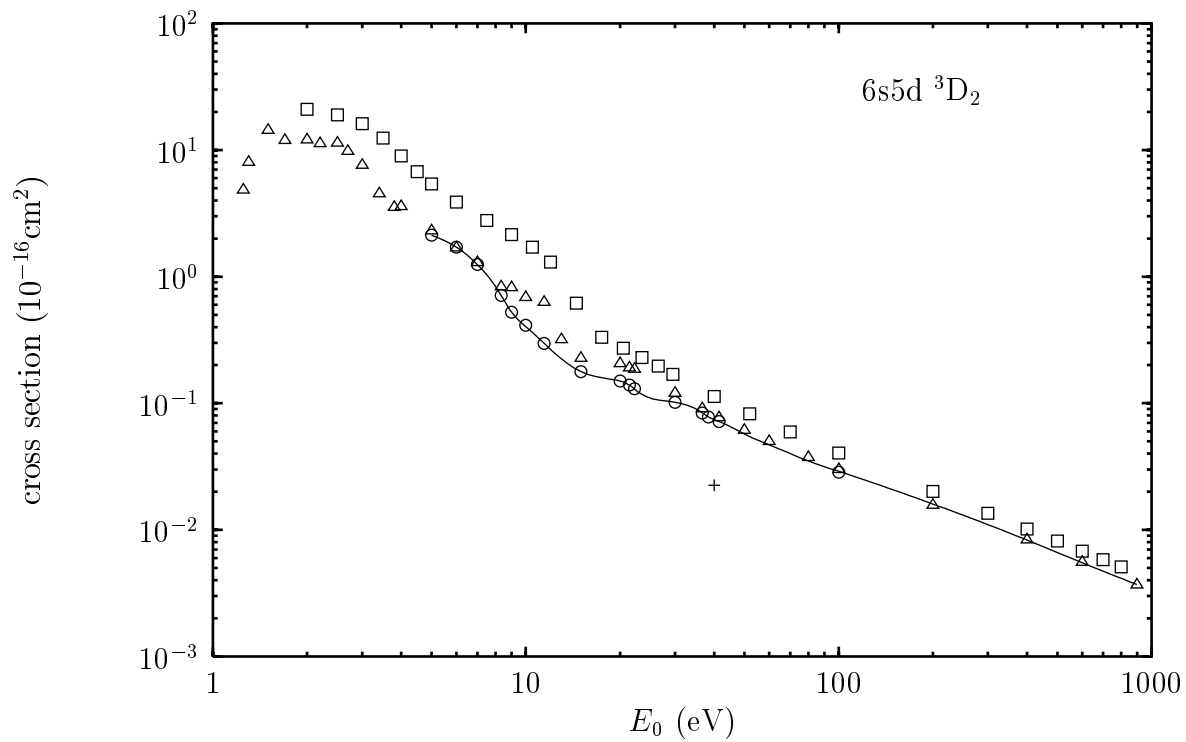


FIG. 20. Same as Fig. 9 except for the 6s5d 3D_2 level.

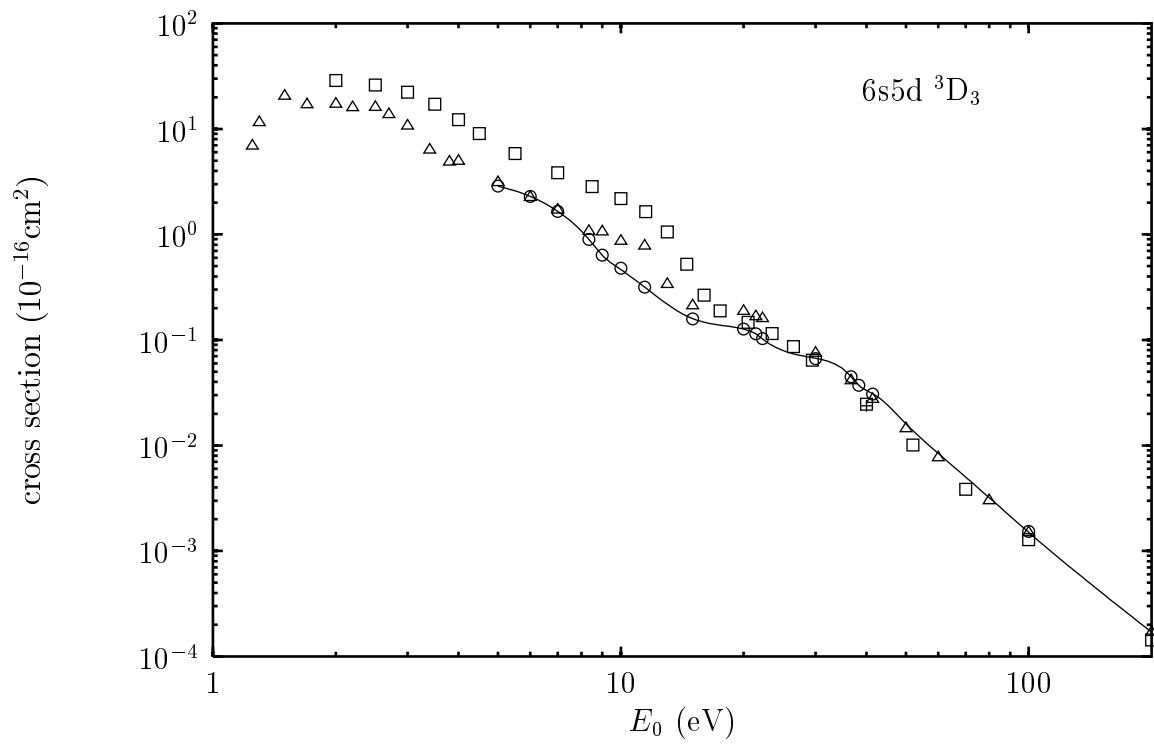


FIG. 21. Same as Fig. 9 except for the $6s5d \ ^3D_3$ level.

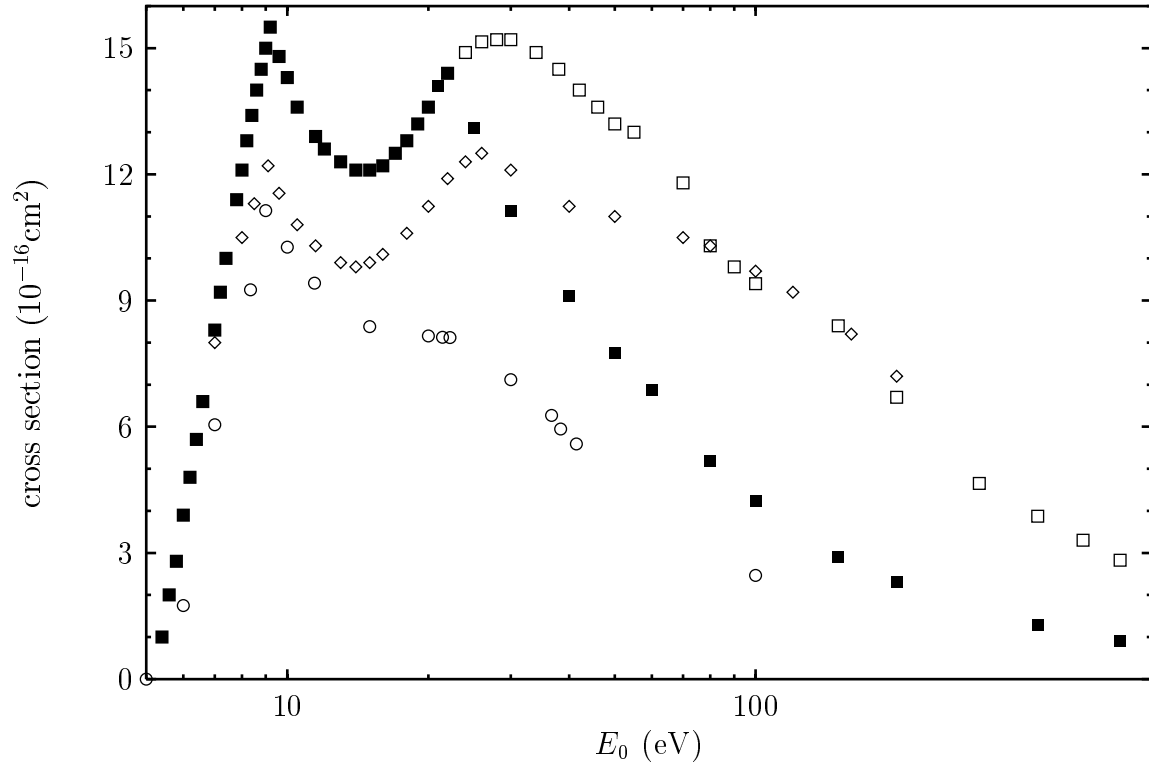


FIG. 22. Ionization cross sections: \circ , CCC (Q^+); \square , (Q_i) and \blacksquare , (Q^+) Dettmann and Karstensen [17]; \diamond , (Q_i) Vainshtein *et al.* [18].

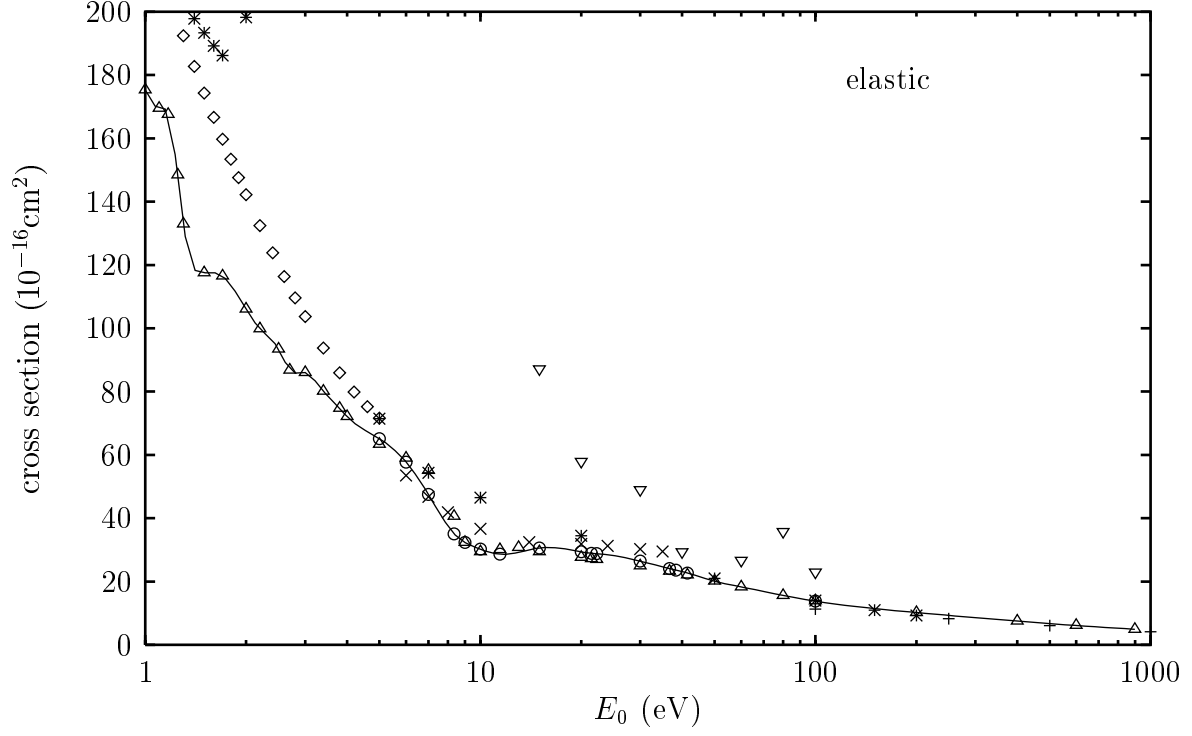


FIG. 23. Integral elastic cross sections: \circ , CCC; \triangle , CC(55); $+$, Gregory and Fink [20]; \times , CC(2) Fabrikant [21]; ∇ , Szymtkowski and Sienkiewicz [24]; \diamond , Yuan and Zhang [22]; $*$, Kelemen *et al.* [25]. The solid line represents our recommended values.

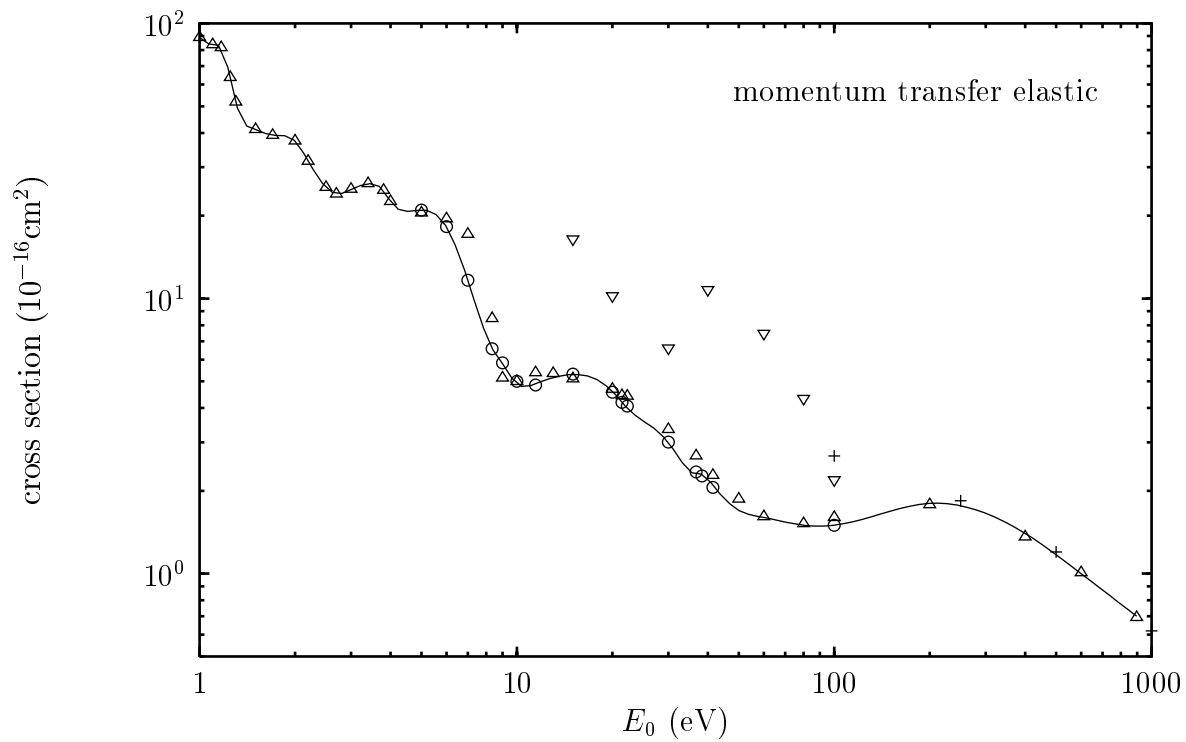


FIG. 24. Same as for Fig. 23 but for momentum transfer cross sections.

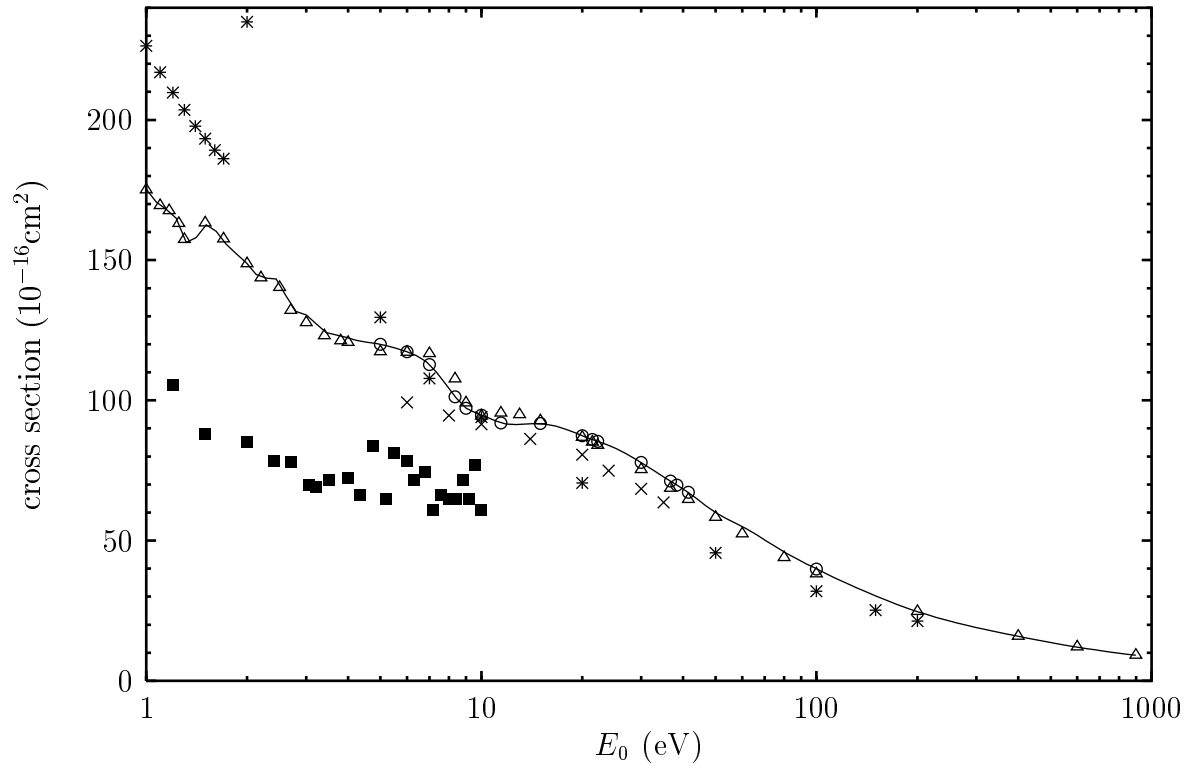


FIG. 25. Total electron scattering cross sections: \circ , CCC; \triangle , CC(55); \times , CC(2) Fabrikant [21]; $*$, Kelemen *et al.* [25]; \blacksquare , Romanyuk *et al.* [19]. The solid line represents our recommended values.